hybrid peptides is controlled by the balance of two driving forces, *i.e.*, the aggregating tendency of alamethicin in the membranes and steric hindrance among the extramembrane segments that prevents excess assembling of the molecules. When the extramembrane segment takes a reduced helical structure, the steric hindrance at the interface between the membranes and H_2O may become smaller. This allows higher numbers of alamethicin molecules to assemble or alters the pore conformation to form a larger pore. The probability of forming channels should also become higher.

4. Conclusion. – This review outlines our approach for designing artificial channel peptides with sensor functions. We have shown that the conformational change in the extramembrane segment can be effectively utilized for channel-current control. The system established here is rather simple and primitive, and would need further development. However, we believe that this concept can be extended to the creation of various ligand-gated ion channels with novel receptor functions as well as artificial sensors. We should also note that we may employ various sensing molecules including oligonucleic acids and synthetic polymers that alter their structures in accordance with external stimuli such as the interactions with ligands.

This work was supported by *Grants-in-Aid for Scientific Research* from the *Ministry of Education, Culture, Sports, Science and Technology of Japan*.

REFERENCES

[1] S. Numa, *Biochem. Soc. Symp.* **1986**, *52*, 119.
[2] A. Miyazawa, Y. Fujiyoshi, N. Unwin, *Nature* **2003**, *423*, 949.
[3] M. Montal, *Curr. Opin. Struct. Biol.* **1996**, *6*, 499.
[4] K. S. Åkerfeldt, J. D. Lear, Z. R. Wassernab, L. A. Chung, W. F. DeGrado, *Acc. Chem. Res.* **1993**, *26*, 191.
[5] S. Futaki, *Biopolymers* **1998**, *47*, 75.
[6] G. A. Woolley, T. Lougheed, *Curr. Opin. Chem. Biol.* **2003**, *7*, 710.
[7] S. Futaki, M. Fukuda, M. Omote, K. Yamauchi, T. Yagami, M. Niwa, Y. Sugiura, *J. Am. Chem. Soc.* **2001**, *123*, 12127.
[8] S. Oiki, W. Danho, V. Madison, M. Montal, *Proc. Natl. Acad. Sci. U.S.A.* **1988**, *85*, 8703.
[9] E. K. O'Shea, R. Rutkowski, P. S. Kim, *Science* **1989**, *243*, 538.
[10] J. A. Zitzewitz, O. Bilsel, J. Luo, B. E. Jones, C. R. Matthews, *Biochemistry* **1995**, *34*, 12812.
[11] G. A. Woolley, B. A. Wallace, *J. Membr. Biol.* **1992**, *129*, 109.
[12] M. S. P. Sansom, *Prog. Biophys. Mol. Biol.* **1991**, *55*, 139.
[13] D. S. Cafiso, *Annu. Rev. Biophys. Biomol. Struct.* **1994**, *23*, 141.
[14] S. Futaki, Y. Zhang, Y. Sugiura, *Tetrahedron Lett.* **2001**, *42*, 1563.
[15] Y. Zhang, S. Futaki, T. Kiwada, Y. Sugiura, *Bioorg. Med. Chem.* **2002**, *10*, 2635.
[16] K. Asami, T. Okazaki, Y. Nagai, Y. Nagaoka, *Biophys. J.* **2002**, *83*, 219.
[17] M. Sakoh, T. Okazaki, Y. Nagaoka, K. Asami, *Biochim. Biophys. Acta* **2003**, *1612*, 117.
[18] T. Okazaki, M. Sakoh, Y. Nagaoka, K. Asami, *Biophys. J.* **2003**, *85*, 267.
[19] T. Okazaki, Y. Nagaoka, K. Asami, *Bioelectrochemistry* **2006**, *71*, 68.
[20] A. Matsubara, K. Asami, A. Akagi, N. Nishino, *Chem. Commun.* **1996**, 2069.
[21] G. A. Woolley, R. M. Epand, I. D. Kerr, M. S. Sansom, B. A. Wallace, *Biochemistry* **1994**, *33*, 6850.
[22] S. You, S. Peng, L. Lien, J. Breed, M. S. Sansom, G. A. Woolley, *Biochemistry* **1996**, *35*, 6225.
[23] D. C. Jaikaran, P. C. Biggin, H. Wenschuh, M. S. Sansom, G. A. Woolley, *Biochemistry* **1997**, *36*, 13873.
[24] A. V. Starostin, R. Butan, V. Borisenko, D. A. James, H. Wenschuh, M. S. Sansom, G. A. Woolley, *Biochemistry* **1999**, *38*, 6144.

[25] D. P. Tieleman, V. Borisenko, M. S. Sansom, G. A. Woolley, *Biophys. J.* **2003**, *84*, 1464.
[26] H. Duclohier, G. Alder, K. Kociolek, M. T. Leplawy, *J. Pept. Sci.* **2003**, *9*, 776.
[27] A. Williams, 'Ion Channels, a Practical Approach', Ed. R. H. Ashley, IRI Press, Oxford, 1995, p. 43–67.
[28] M. Montal, P. Mueller, *Proc. Natl. Acad. Sci. U.S.A.* **1972**, *69*, 3561.
[29] E. K. O'Shea, R. Rutkowski, W. F. Stafford III, P. S. Kim, *Science* **1989**, *245*, 646.
[30] T. Kiwada, K. Sonomura, Y. Sugiura, K. Asami, S. Futaki, *J. Am. Chem. Soc.* **2006**, *128*, 6010.
[31] I. Hamachi, Y. Yamada, T. Matsugi, S. Shinkai, *Chem.–Eur. J.* **1999**, *5*, 1503.
[32] S. Futaki, T. Kiwada, Y. Sugiura, *J. Am. Chem. Soc.* **2004**, *126*, 15762.
[33] N. Sakai, J. Mareda, S. Matile, *Acc. Chem. Res.* **2005**, *38*, 79.
[34] H. Bayley, L. Jayasinghe, *Mol. Membr. Biol.* **2004**, *21*, 209.
[35] G. W. Gokel, P. H. Schlesinger, N. K. Djedovic, R. Ferdani, E. C. Harder, J. Hu, W. M. Leevy, J. Pajewska, R. Pajewski, M. E. Weber, *Bioorg. Med. Chem.* **2004**, *12*, 1291.
[36] S. Futaki, Y. Zhang, T. Kiwada, I. Nakase, T. Yagami, S. Oiki, Y. Sugiura, *Bioorg. Med. Chem.* **2004**, *12*, 1343.
[37] B. A. Cornell, V. L. B. Braach-Maksvytis, L. G. King, P. D. J. Osman, B. Raguse, L. Wieczorek, R. J. Pace, *Nature* **1997**, *387*, 580.
[38] P. Talukdar, G. Bollot, J. Mareda, N. Sakai, S. Matile, *Chem.–Eur. J.* **2005**, *11*, 6525.

Received December 22, 2006

THE JOURNAL OF BIOLOGICAL CHEMISTRY VOL. 282, NO. 43, pp. 31643–31655, October 26, 2007
Printed in the U.S.A.

Growth Factor Induction of Cripto-1 Shedding by Glycosylphosphatidylinositol-Phospholipase D and Enhancement of Endothelial Cell Migration*[S]

Received for publication, March 29, 2007, and in revised form, August 21, 2007 Published, JBC Papers in Press, August 24, 2007, DOI 10.1074/jbc.M702713200

Kazuhide Watanabe[‡], Caterina Bianco[‡], Luigi Strizzi[‡], Shin Hamada[‡], Mario Mancino[‡], Veronique Bailly[§], Wenjun Mo[§], Dingyi Wen[§], Konrad Miatkowski[§], Monica Gonzales[‡], Michele Sanicola[§], Masaharu Seno[¶], and David S. Salomon[‡1]

From the [‡]Tumor Growth Factor Section, Mammary Biology & Tumorigenesis Laboratory, Center for Cancer Research, NCI, National Institutes of Health, Bethesda, Maryland 20892, [§]Biogen Idec Inc., Cambridge, Massachusetts 02142, and the [¶]Department of Medical and Bioengineering Science, Graduate School of Natural Science and Technology, Okayama University, Okayama 700-8530, Japan

Cripto-1 (CR-1) is a glycosylphosphatidylinositol (GPI)-anchored membrane glycoprotein that has been shown to play an important role in embryogenesis and cellular transformation. CR-1 is reported to function as a membrane-bound co-receptor and as a soluble ligand. Although a number of studies implicate the role of CR-1 as a soluble ligand in tumor progression, it is unclear how transition from the membrane-bound to the soluble form is physiologically regulated and whether differences in biological activity exist between these forms. Here, we demonstrate that CR-1 protein is secreted from tumor cells into the conditioned medium after treatment with serum, epidermal growth factor, or lysophosphatidic acid, and this soluble form of CR-1 exhibits the ability to promote endothelial cell migration as a paracrine chemoattractant. On the other hand, membrane-bound CR-1 can stimulate endothelial cell sprouting through direct cell-cell interaction. Shedding of CR-1 occurs at the GPI-anchorage site by the activity of GPI-phospholipase D (GPI-PLD), because CR-1 shedding was suppressed by siRNA knockdown of GPI-PLD and enhanced by overexpression of GPI-PLD. These findings describe a novel molecular mechanism of CR-1 shedding, which may contribute to endothelial cell migration and possibly tumor angiogenesis.

The Epidermal Growth Factor-Cripto-1/FRL-1/Cryptic (EGF-CFC)[2] family of genes, including mammalian *Cripto-1* (*CR-1/Tdgf1*), has been shown to play an important role in vertebrate development and in tumor progression (1). EGF-CFC proteins are indispensable for early embryonic development, being involved in the formation of the primitive streak, patterning of the anterior/posterior axis, mesoendoderm formation, and establishment of left-right asymmetry (2). *CR-1* is an oncofetal gene, which is expressed during early developmental stages and is re-expressed in several types of human carcinomas (3). In fact, CR-1 protein is highly expressed in a number of human carcinomas, including breast (75–82%), colon (67–84%), and gastric cancer (33–47%), where it is being assessed as a tumor-specific target for immunotherapy (3, 4). Mice that overexpress a human CR-1 transgene selectively in mammary epithelium develop mammary hyperplasia and adenocarcinomas (5–7). Conversely, blockade of CR-1-mediated signaling suppresses tumor growth (4, 8, 9).

CR-1 functions through at least three different signaling pathways: 1) as a co-receptor for the transforming growth factor β-related proteins Nodal and growth and differentiation factors 1 and 3 (10–12), 2) as a ligand for glypican-1/c-Src/MAPK/PI3K-Akt signaling (13), and 3) as an inhibitor for activin/transforming growth factor-β signaling (8, 14). Nodal requires EGF-CFC proteins as co-receptors to bind the activin type I receptors (activin-like kinases 4 and 7) and activin type II receptor (ActRII). Embryological defects in CR-1-null mice are lethal mainly due to a disruption of Nodal-dependent signaling (15). CR-1 can also function independently of Nodal as a ligand for glypican-1, which can activate a c-Src/MAPK/PI3K-Akt intracellular signaling pathway (3) and then promote cell proliferation, survival, migration, and invasion (5). Some of the oncogenic actions of CR-1, such as tumor angiogenesis, utilize this latter pathway (16).

EGF-CFC proteins contain several domains that include an N-terminal signal peptide, a variant EGF-like domain, a

* This work was supported by National Institutes of Health Intramural Funding. The costs of publication of this article were defrayed in part by the payment of page charges. This article must therefore be hereby marked "*advertisement*" in accordance with 18 U.S.C. Section 1734 solely to indicate this fact.

[S] The on-line version of this article (available at http://www.jbc.org) contains supplemental Figs. S1–S3.

[1] To whom correspondence should be addressed: Tumor Growth Factor Section, Mammary Biology & Tumorigenesis Laboratory, Center for Cancer Research, NCI, National Institutes of Health, Bldg. 37, Rm. 1118B, 37 Convent Drive, Bethesda, MD 20892-4254. Tel.: 301-496-9536; Fax: 301-402-8656; E-mail: salomond@mail.nih.gov.

[2] The abbreviations used are: EGF-CFC, epidermal growth factor-Cripto-1/FRL-1/Cryptic; ADAM, a disintegrin and metalloproteinase domain; CR-1, Cripto-1; CTxB, Cholera toxin B; DRMs, detergent-resistant microdomains; EGFR, EGF receptor; EV, empty vector; FBS, fetal bovine serum; GPI, glycosylphosphatidylinositol; GPI-PLD, GPI-phospholipase D; HRP, horseradish peroxidase; HUVEC, human umbilical vein epithelial cell; IL-6, interleukin-6; LPA, lysophosphatidic acid; mAb, monoclonal antibody; MS, mass spectrometry; MS/MS, tandem mass spectrometry; PKC, protein kinase C; PLC-γ, phospholipase C γ; PMA, phorbol 12-myristate 13-acetate; PNT, 1,10-phenanthroline; SRM, suramin; TfR, transferrin receptor; MES, 2-(*N*-morpholino)ethanesulfonic acid; MAPK, mitogen-activated protein kinase; PI3K, phosphatidylinositol 3-kinase; DAPI, 4′,6-diamidino-2-phenylindole; FACS, fluorescence-activated cell sorting; siRNA, small interference RNA; RT, reverse transcription.

cysteine-rich CFC domain, and a glycosylphosphatidylinositol (GPI)-linkage signal at the C-terminus. CR-1 is tethered to the outer leaflet of the plasma membrane via a GPI anchor (17). Although the GPI anchoring enables CR-1 to act as a membrane-bound co-receptor, CR-1 can also be released as a soluble protein (18, 19). However, the endogenous regulatory mechanism controlling CR-1 shedding is largely unknown.

We have previously found that CR-1 is a potent endothelial chemoattractant *in vitro* and promotes tumor angiogenesis *in vivo* (16). To facilitate endothelial cell migration *in vivo*, CR-1 should be released from tumor cells to interact with surrounding endothelial cells. In this respect, a recent study has demonstrated that the plasma levels of CR-1 in breast and colon cancer patients were significantly higher than those of healthy controls (20), suggesting that CR-1 is released into plasma from tumor cells and that plasma CR-1 levels might serve as a surrogate tumor marker. Therefore, shedding of CR-1 is a key biological process in understanding the characteristics of CR-1 as a diagnostic and therapeutic target in cancer and in delineating the mechanism by which CR-1 can initiate angiogenesis. In the current study, we have evaluated the differential roles of membrane-bound and soluble forms of CR-1 in stimulating endothelial cells and delineated the mechanism of CR-1 shedding *in vitro*.

EXPERIMENTAL PROCEDURES

Cells—HEK293T (293T), MDCK, COS7, and SW480 cells (ATCC, Manassas, VA) were maintained in Dulbecco's modified Eagle's medium supplemented with 10% fetal bovine serum (FBS). NTERA2/D1 cells (ATCC) were grown in Macoy's 5A medium with 15% FBS. Human umbilical vein endothelial cells (HUVECs) were cultured as described previously (16, 21). Human embryonic cells Per-C6 (Crucell, Leiden, The Netherlands) transfected with wild-type CR-1 were grown in Dulbecco's modified Eagle's medium containing 10 mM $MgCl_2$, 0.5 mg/ml G418, and 10% FBS.

Reagents—Human CR-1 monoclonal antibodies (mAbs) (MAB2771 and FAB2772P) were obtained from R&D Systems (Minneapolis, MN) or developed as previously reported (B3F6) (8). Rabbit polyclonal anti-CR-1 antibody was previously described (20). Antibodies against total p42/44 MAPK, phospho-p42/44 MAPK, total Akt, phospho-Akt, and phospho-Smad2 were obtained from Cell Signaling (Danvers, MA), total Smad2 from Upstate (Chicago, IL), β-actin from Sigma-Aldrich, and transferrin receptor (TfR) and V5 from Invitrogen. Phosphatidylinositol-phospholipase C (PI-PLC) and horseradish peroxidase (HRP)-conjugated Cholera toxin B (CTxB) were purchased from Sigma-Aldrich. All fluorescent dyes were purchased from Invitrogen, and all chemical compounds were from Calbiochem (Darmstadt, Germany) or, for recombinant proteins, from R&D Systems. Lysophosphatidic acid (LPA) was purchased from Avanti Polar Lipids (Alabaster, AL). All other reagents were purchased from Sigma-Aldrich unless otherwise indicated.

Plasmids and Transfection—The cDNA encoding the open reading frame of human CR-1 was cloned from NTERA2/D1 cells (13). All CR-1-related constructs were generated by PCR-based methods and cloned into the pCI neo vector (Promega, Madison, WI). The stop codon (TGA) was inserted just after Ser-161 or Ser-169 of the full-length CR-1 (amino acids 1–188, CR1WT) to obtain CR1ΔC (Ser-161) or (Ser-169), respectively. The transmembrane portion of ErbB4 (amino acids 651–683) with a FLAG tag was inserted after Ser-169 of CR1WT to obtain CR1TM. The cDNA encoding mouse GPI-phospholipase D (GPI-PLD) was purchased from ATCC (IMAGE clone, 5052822). The open reading frame with Kozak sequence was amplified by PCR using primers: F, ACCATGTCTGCAGGCAGGCTGTGG; R, GTCTGAGCTGAAGCTGTAGAC. The PCR product was cloned into pEF6/V5-His TOPO TA expression vector (Invitrogen) in-frame to generate a C-terminal-tagged mGPIPLD-V5 expression vector. DNA sequences were validated by direct sequencing. Transfections were performed using Lipofectamine 2000 (Invitrogen). To establish stable transfectants, transfected cells were selected by G418, at a concentration of 1 mg/ml for 293T and MDCK cells and 2 mg/ml for SW480 cells, respectively.

Isolation of Detergent-resistant Microdomains—DRM isolation by nonionic detergent Triton X-100 was performed as previously reported (22). NTERA2/D1 cells were washed with cold phosphate-buffered saline and scraped into 2 ml of MBS (MES-buffered saline; 25 mM MES, pH 6.5, 0.15 M NaCl) containing 1% Triton X-100 and solubilized for 20 min at 4 °C. After homogenization by 10 strokes with a tight-fitting Dounce homogenizer, samples were adjusted to 40% sucrose by addition of 2 ml of 80% sucrose. Then, a 5–40% discontinuous sucrose gradient was formed and centrifuged at 40,000 rpm for 20 h, in an SW40Ti rotor (Beckmann-Coulter, Fullerton, CA). Twelve 1-ml fractions were removed from the top of the tubes and analyzed by Western blotting for CR-1 and for the non-raft-associated membrane protein, TfR using an anti-human TfR antibody (1:2,000) and by dot blotting for the lipid raft marker GM-1 using HRP-conjugated CTxB (1:1,000).

Phase Separation—Phase separation by Triton X-114 was performed as previously described (23). Cells were lysed in lysis buffer (150 mM NaCl, 50 mM Tris-HCl, pH 8.0, 1% Nonidet P-40, 0.5% deoxycholic acid) with Complete protease inhibitor (Roche Applied Science), and PI-PLC treatment was performed by incubating with 1 unit/ml PI-PLC (Sigma-Aldrich) for 30 min at 37 °C. Cell lysates and conditioned media were then adjusted to 2% Triton X-114 using 2× Triton X-114 solution (40 mM Tris-HCl, pH 8.0, 300 mM NaCl, 4% Triton X-114). After incubation for 1 h on ice, phase separation was carried out by warming up to 37 °C and subsequent centrifugation at 10,000 × *g*, 25 °C. Before applying for Western blotting, proteins were precipitated with chloroform-methanol precipitation to remove the detergent.

Western Blot Analysis—Western blot analysis was performed using 4–20% gradient SDS-PAGE gels (Invitrogen), and CR-1 protein was detected with B3F6 mAb at a 1:5,000 dilution and anti-mouse IgG HRP-conjugated secondary antibody (1:3,000, Amersham Biosciences) (supplemental Fig. S1, *A–C*). For quantification, 50 μg of total cell lysates and 40 μl of conditioned media were analyzed for NTERA2/D1 cells, and 20 μg of total cell lysates and 20 μl of conditioned media were analyzed

for 293T transfectants, respectively. All images of Western blot analysis in this work were visualized, processed, and quantified with an Image Analyzer equipped with LabWorks software (Ultra Violet and Laboratory Products, Upland, CA).

Enzyme-linked Immunosorbent Assays—A sandwich-based enzyme-linked immunosorbent assay was performed as previously described (20) with minor modifications. Anti-CR-1 mAb B3F6 (1 μg/well) was absorbed to a 96-well Nunc-Immuno Maxisorp Plate (Nunc, Roskilde, Denmark). The plates were blocked with blocking solution (Kirkegaard & Perry Laboratories, Gaithersburg, MD), washed with wash buffer (Kirkegaard & Perry Laboratories), and incubated overnight at 4 °C with 50 μl of conditioned media from growth factor-treated cells. Human CR-1 recombinant protein (R&D Systems) was used as a standard (supplemental Fig. S1, *D* and *E*). After washing, a rabbit polyclonal anti-CR-1 antibody (1:3,000) was added to the plates for 1 h at room temperature. The plates were then washed five times with washing buffer and incubated with anti-rabbit IgG HRP-conjugated antibody (1:3,000, Amersham Biosciences) for 1 h at room temperature. The plates were developed with 3,3′,5,5′-tetramethylbenzidine peroxidasesubstrate (Kirkegaard & Perry Laboratories), and reactions were quenched with stop solution (Kirkegaard & Perry Laboratories). Absorbance was read at 450 nm.

Fluorescence Imaging—Cells were grown for overnight in chambered slides. After washing with phosphate-buffered saline, cells were fixed in 4% paraformaldehyde. Depending on the experiment, cells were permeabilized with 0.2% Triton X-100. After blocking, CR-1 was labeled with 5 μg/ml MAB2771 and detected with Alexa Fluor 488-conjugated secondary antibody (Invitrogen). Plasma membrane and lipid rafts were detected with 5 μg/ml wheat germ agglutinin-Alexa Fluor 594 conjugate and with 1 μg/ml CTxB-Alexa Fluor 594 conjugate (Invitrogen), respectively. Prolong Gold Antifade reagent with DAPI (Invitrogen) was used as a mounting medium. For confocal images, a Zeiss LSM 510 NLO Meta confocal system (Carl Zeiss, Göttingen, Germany) with an Axiovert 200M inverted microscope equipped with a 63× numerical aperture 1.4 Plan-Apochromat oil immersion objective lens was used. Z stacks were collected with Zeiss AIM software using a multitrack configuration.

FACS Analysis—293T transfectants were collected with phosphate-buffered saline containing 4 mM EDTA. After washing with ice-cold FACS buffer (phosphate-buffered saline with 0.1% bovine serum albumin), 1.0×10^5 cells were incubated for 20 min with anti-human CR-1 phycoerythrin-conjugated antibody (FAB2772P) at a dilution of 1:50. Cells were then pelleted, resuspended in 500 μl of ice-cold FACS buffer, and analyzed using a FACScan instrument (BD Biosciences).

Migration Assay—Transwell migration assay of HUVECs was performed as previously described (21) with some modifications. Briefly, 24 h prior to the assay, the culture medium of 293T or SW480 transfectants, which were seeded in the bottom chamber, were replaced with serum-free medium with or without growth factors or chemicals. 5×10^4 serum-starved HUVECs were seeded in the upper chamber of 8-μm pore filter 24-well Transwell plates (Corning, Acton, MA). After 12–16 h, cells were fixed and stained, and cells on the upper side of the filters were wiped away with cotton swabs. Migrated cells on the bottom side of the filter were quantified using IMAGE (National Institutes of Health) software. Each experiment was performed in triplicates and repeated at least twice in independent culture conditions.

Direct Co-culture Assay—HUVECs were labeled with CellTracker green 5-chloromethylfluorescein diacetate (Invitrogen) prior to the assay. 5×10^4 labeled HUVECs were seeded on confluent cultures of 293T transfectants that had been grown in 6-well plates in serum-free medium. After 12–16 h, cells were fixed and counter staining was performed with rhodamine-conjugated phalloidin (Invitrogen) and DAPI. Images were taken by fluorescence microscopy, on an IX51 inverted microscope equipped with a 20× 0.4-nemerical aperture objective lens (Olympus, Tokyo, Japan). For quantification, HUVECs with sprouting morphology (spindle shapes and/or processes) were counted in total 70–135 CellTracker-positive HUVECs/field under low power magnification. Counting was performed for three different fields in a blinded manner, and three independent experiments were performed.

siRNA and RT-PCR Analysis—siRNAs against GPI-PLD were purchased from Ambion (Foster City, CA). Sequences are as below follows: siGPIPLD1 sense, GGAUUCCUUAGGACCAUGGtt; antisense, CCAUGGUCCUAAGGAAUCCtt; siGPIPLD2 sense, GCUAUUGAUUUUCACGGCUtt; antisense, AGCCGUGAAAAUCAAUAGCTC; siGPIPLD3 sense, GCUCUGGAGUUUCUUCAGCtt; and antisense, GCUGAAGAAACUCCAGAGCtc. These sequences contain 1- to 4-nucleotide mismatches with mouse GPI-PLD, which was used for the rescue experiment. Mixture of nonspecific Control siRNAs #1, #2, and #3 (Dharmacon, Chicago, IL) were used for a negative control. Subconfluent 293T or SW480 cells were transfected with a total of 30 μM siRNAs using Lipofectamine 2000. Because the knockdown efficiencies of each siRNA were not sufficient (<50% inhibition), we used a mixture of three siRNAs and achieved a maximum inhibition of >70%. RT-PCR was performed using Supermix (Invitrogen) according to manufacturer's instructions at the indicated cycles. A PCR primer set for human GPI-PLD was purchased from Superarray (Frederick, MD).

Mass Spectrometric Analysis of Released CR-1—The cultured media from CR-1-transfected Per-C6 cells was harvested and clarified, and the released CR-1 protein was affinity-purified by binding to the B3F6 mAb coupled to CNBr-activated Sepharose.

Deglycosylation, Reduction, and Alkylation of Shed CR-1—*N*-Linked glycans were removed from the protein with peptide *N*-glycosidase F. About 1.5 μl of peptide *N*-glycosidase F (2.5 milliunits/μl, Prozyme, San Leandro, CA) was added to 40 μl of a solution containing ~10 μg of protein. The solution was incubated at 37 °C overnight. The deglycosylated protein was then reduced with 40 mM dithiothreitol in 6 M guanidine hydrochloride for 2 h at 37 °C, and alkylation was done by adding 0.5 μl of 4-vinylpyridine into 50 μl of the solution. The solution was incubated at room temperature in the dark for 60 min. The alkylated proteins were recovered by precipitation with 40 volumes of −20 °C ethanol. The solution was stored at −20 °C for

1 h and then centrifuged at 14,000 × *g* for 8 min at 4 °C. The supernatant was discarded, and the precipitate was washed once with −20 °C ethanol.

Trypsin Digestion—About 10 μg deglycosylated and alkylated protein was digested with 7% (w/w) of trypsin (Promega) in 1 M urea, 0.2 M Tris-HCl, pH 8.0, 1 mM $CaCl_2$, for 5 h at room temperature; the final volume was 50 μl.

Separation and Analysis of the Digested Shed CR-1 Protein—The tryptic digest was analyzed on an liquid chromatography-MS/MS system composed of a nano-flow high-performance liquid chromatograph (Dionex, Sunnyvale, CA) and a QSTAR XL mass spectrometer (Applied Biosystems). The high-performance liquid chromatograph was equipped with a 0.3-mm × 1-mm Pepmap C18-trap column for desalting and a 0.075-mm × 150-mm, 100-Å, Pepmap C18 column for separation. Peptides were eluted with a 70-min linear gradient (0–50% acetonitrile) in 0.03% trifluoroacetic acid at a flow rate of 200 nl/min. MS and MS/MS spectra were acquired using information-dependent acquisition and switched automatically between MS and MS/MS. The nanoelectrospray was generated with a nanoelectrospray ionization source (Protana, Toronto, Canada) using a PicoTip needle (15-μm inner diameter, New Objectives, Woburn, MA) maintained at a voltage of 1700 V. MS/MS spectra were collected in the *m/z* range of 50–2,200, and the collision energy setting was automatically determined by the information-dependent acquisition based on the *m/z* values of each precursor ion.

Statistical Analysis—Student's *t* test was used to determine the statistical significance of the quantitative results. Results with a *p* value of <0.05 were considered statistically significant.

RESULTS

CR-1 Localization in Lipid Rafts—The GPI-anchorage of CR-1 to the cell membrane has been previously reported by the ability of bacterial PI-PLC to release CR-1 from cultured cells (17). We further demonstrated that CR-1 exhibits pericellular characteristics of a GPI-anchored protein in that CR-1 can be localized to lipid raft domains on the plasma membrane by immunocytochemical analysis in human embryonal carcinoma NTERA2/D1 cells, from which CR-1 was isolated and cloned and is expressed at a relatively high level (1). CR-1 exhibited a punctate staining pattern, a proportion of which was co-localized with the lipid raft marker GM-1, which has been labeled with CTxB (Fig. 1*A*). To confirm the results from imaging analysis, biochemical isolation of DRMs was performed in NTERA2/D1 cells. Detergent resistance has been considered as a biochemical characteristic of lipid rafts (24). CR-1 protein was found to be enriched in DRMs, which contain GM-1 but do not contain a non-raft membrane protein TfR (25), although a more substantial amount of immunoreactive CR-1 was found to be associated in the soluble fractions (*fractions 9–12*, Fig. 1*B*).

Because apical sorting is one of the well known characteristics of GPI-anchored proteins, we examined the CR-1 localization in a well established model of cell polarity, MDCK cells (26). In fully polarized MDCK cells stably transfected with CR-1, CR-1 was stained mainly on the apical surface (supplemental Fig. S2*A*). A substantial amount of CR-1 protein was detected in the conditioned medium obtained from the apical side but not from the basal side in CR-1-expressing MDCK cells (supplemental Fig. S2*B*). These results suggest that CR-1 is sorted to the apical side of the plasma membrane in polarized epithelial cells.

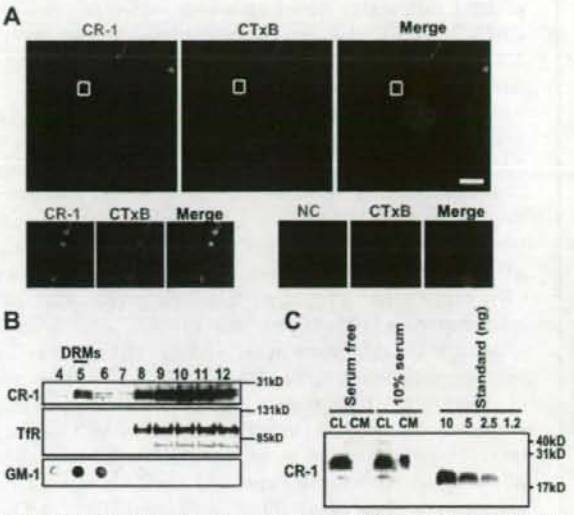

FIGURE 1. **Lipid raft localization and release of CR-1 protein.** *A*, NTERA2/D1 cells were stained with anti-CR-1 mAb (*green*), and lipid raft marker GM-1 was labeled with CTxB (*red*) without permeabilization and analyzed by confocal microscopy (*upper panel*). Magnified images for the marked regions in the *upper panel* are shown in the *lower left panel*. Negative controls without primary antibody are shown in the *lower right panel*. Nuclei were stained with DAPI (*blue*) in all merged images. *Scale bar* = 10 μm. *B*, biochemical isolation of DRMs with 1% Triton X-100 by sucrose-gradient centrifugation of NTERA2/D1 cells. The gradient fractions (*lanes 4–12*) were analyzed with Western blot analysis for CR-1. Transferrin receptor (*TfR*) was used as a control for non-raft membrane protein. The lipid raft marker *GM-1* in the same samples was detected with HRP-conjugated CTxB by dot-blot analysis. *C*, comparative study of cell-associated (*CL*) and released (*CM*) CR-1 with or without serum by semi-quantitative Western blot analysis (see Table 1 and supplemental Fig. S1, *A–C*). A representative blot for NTERA2/D1 cells is shown. The indicated amount of recombinant human CR-1 protein was used as a standard.

TABLE 1
Semi-quantitative analysis of cell-associated and released CR-1

	Cell extracts		Conditioned media	
	ng/1 μg total protein		*ng/ml*	
293T CR1WT (serum-free)	~1.3		~36	
293T CR1WT (10% serum)	~1.4	~1.1-fold	>500	>14-fold
NTERA2/D1 (serum-free)	~0.16		~4	
NTERA2/D1 (10% serum)	~0.18	~1.1-fold	~130	~32-fold

293T CR1WT cells or NTERA2D1 cells were cultured for 24 h with indicated conditions. The amounts of released and cell-associated CR-1 were quantified by Western blot analysis (see Fig. 1*C* and supplemental Fig. S1, *A–C*) and compared to standard amounts of recombinant CR-1 after densitometric scanning. Values represent average of four independent experiments.

Regulation of CR-1 Shedding by Serum and Growth Factors—To evaluate the extent of CR-1 secretion into the medium, we compared the amount of released and cell-associated CR-1 by semi-quantitative Western blot analysis using recombinant human CR-1 protein as a standard (Table 1, Fig. 1*C*, and supplemental Fig. S1, *A–C*). As summarized in Table 1, when cells were cultured in serum-free medium, little CR-1 protein was detected in the conditioned medium

of 293T cells stably transfected with wild-type CR-1 (293T CR1WT cells) and in the conditioned medium from NTERA2/D1 cells that express endogenous CR-1 (~36 ng/ml and ~4 ng/ml, respectively). However, when these cells were cultured in the presence of 10% serum, a higher amount of CR-1 was detected in the conditioned media from 293T and NTERA2/D1 cells (>500 ng/ml and ~130 ng/ml, respectively), which represents >14- and ~32-fold increase in comparison with release of CR-1 under serum-free conditions. These concentrations of CR-1 in the medium are comparable with the concentration of exogenous recombinant CR-1 protein that is required to induce several different cellular responses (100–200 ng/ml) (13).

Because the difference in cell viability after 24-h cultures, in the presence or absence of serum, could affect the amount of released CR-1 protein in the conditioned medium, we evaluated the short term effect of serum on shedding of CR-1. Heat-inactivated serum in which a number of heat-labile lipases and proteinases had been inactivated could induce an increase of >3-fold in shedding of CR-1 in SW480 colon carcinoma cells transfected with wild-type CR-1 expression vector (SW480 CR1 cells) within 30 min (Fig. 2*A*). SW480 colon carcinoma cells were selected because this cell line expresses low amounts of endogenous CR-1 (1, 3). The effect of heat-inactivated serum was also observed in other cell types, such as 293T CR1WT and in NTERA2/D1 cells that express native CR-1 (data not shown). This effect of serum is dependent on phospholipase Cγ (PLCγ) and protein kinase C (PKC), because serum-induced CR-1 shedding was inhibited in a dose-dependent manner by the PLCγ inhibitor U73122 (Fig. 2*B*) and by the PKC-specific inhibitor GF109203X, respectively (Fig. 2*C*). Phorbol 12-myristate 13-acetate (PMA), which is known to activate diacylglycerol-dependent PKCs, was able to mimic the effect of serum on facilitating CR-1 shedding by nearly 3-fold in both 293 CR1WT cells (data not shown) and SW480 CR1 cells (Fig. 2*D*).

These findings strongly suggest that serum factor(s) can induce CR-1 shedding through activation of PLCγ and PKC. To identify endogenous regulatory factors that might enhance CR-1 shedding from cells and that might be present in serum, the levels of released CR-1 were examined after stimulation of 293T CR1WT and SW480 CR1 cells with different growth factors and cytokines using an enzyme-linked immunosorbent assay (Table 2). We found that nine distinct growth factors, including EGF, heparin binding-EGF, hepatocyte growth factor, fibroblast growth factor-2, LPA, interleukin-6 (IL-6), IL-8, tumor necrosis factor α, and interferon γ, significantly stimulated CR-1 shedding. Some of the factors, including LPA, IL-6, and IL-8 had cell-type-specific effects. For example, LPA strongly induced CR-1 shedding in SW480 CR1 cells but had no significant effect on CR-1 shedding in 293T CR1WT cells.

Growth Factors Induce Endothelial Cell Migration by Enhancing CR-1 Shedding—Because EGF and LPA are involved in stimulating tumor progression and tumor angiogenesis (27, 28), and because CR-1 has also been shown to stimulate angiogenesis (16), we hypothesized that these factors might induce endothelial cell migration by facilitating the release of CR-1 from the tumor cell membrane. The effect of LPA and EGF was therefore examined on SW480 colon cancer cells. The induction of CR-1 shedding by LPA or EGF in transfected SW480 CR1 cells that had been grown in serum-free medium was confirmed by Western blot analysis (Fig. 3*A*). CR-1 shedding induced by LPA or EGF was inhibited by the PKC inhibitor

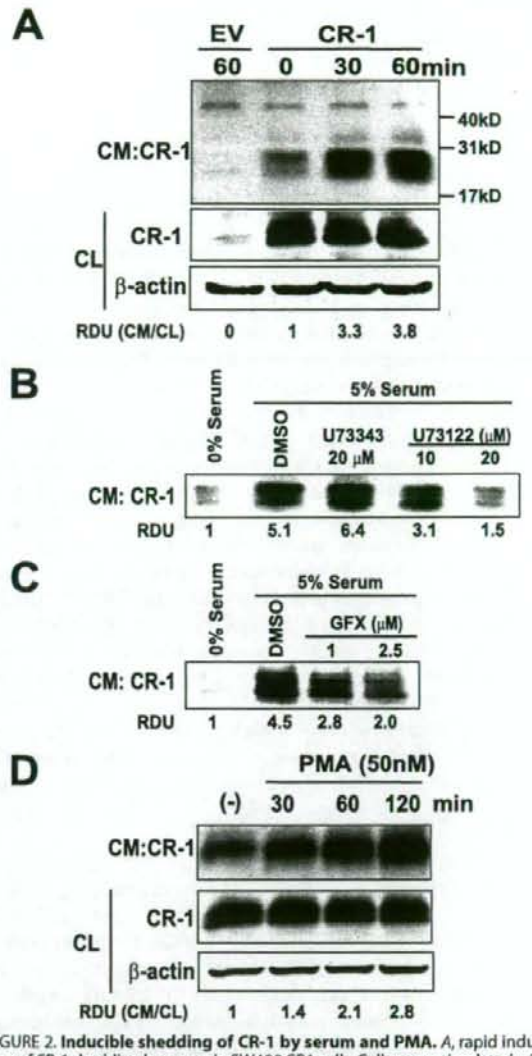

FIGURE 2. **Inducible shedding of CR-1 by serum and PMA.** *A*, rapid induction of CR-1 shedding by serum in SW480 CR1 cells. Cells were stimulated with 5% FBS for 0–60 min. Released CR-1 in the conditioned medium (*CM*) and cell-associated CR-1 in total cell lysates (*CL*) were evaluated by Western blot analysis. *EV*, empty vector; *RDU*, relative densitometry unit. *B* and *C*, effect of U73122 or GF109203X (*GFX*) on serum-induced CR-1 shedding. SW480 CR1 cells were treated with or without 5% serum for 30 min with the indicated dose of indicated chemicals, and released CR-1 in the conditioned medium was analyzed by Western blotting. Cells were pretreated with chemicals 30 min before the treatment with serum. Me_2SO (*DMSO*) was used for vehicle controls. U73343 was used for a negative control analogue for U73122. *D*, CR-1 release by PMA. SW480 CR1 cells were stimulated with 50 nM PMA for 0–120 min. Released (*CM*) and cell-associated CR-1 (*CL*) was analyzed by Western blotting.

TABLE 2

Effect of growth factors on CR-1 shedding

293T CR1WT cells or SW480 CR1WT cells were stimulated for 6–8 h with the indicated factors (EGF, HB-EGF, FGF-2, HGF, IL-6, and TNFα, 50 ng/ml; LPA; 5 μM; IL-8, 100 ng/ml; and IFNγ, 10 ng/ml). After stimulation, conditioned medium was collected and enzyme-linked immunosorbent assay was performed as described under "Experimental Procedures." Values represent average (ng/ml) ± S.D. of four independent experiments.

	293T CR1WT cells	SW480 CR1WT cells
Control	12.6 ± 5.7	8.5 ± 1.8
EGF	55.3 ± 8.1*	43.3 ± 6.7*
HB-EGF	59.4 ± 16.0*	44.7 ± 5.7*
FGF-2	58.0 ± 18.4*	27.6 ± 3.2*
HGF	52.6 ± 14.6*	25.5 ± 2.2*
LPA	7.7 ± 3.5	56.8 ± 11.6*
IL-6	39.2 ± 11.3*	12.8 ± 4.2
IL-8	12.4 ± 4.1	28.6 ± 8.0*
TNFα	60.4 ± 19.0*	39.2 ± 13.2*
IFNγ	41.0 ± 12.3*	30.0 ± 10.0*

*$p < 0.05$ compared with control by Student's *t*-test.

GF109203X (data not shown), suggesting that these factors utilize a pathway similar to that induced by serum and by PMA.

We then evaluated the biological response of CR-1 shedding induced by EGF and LPA in facilitating HUVEC migration. EGF or LPA had weak direct effects on endothelial cell migration unlike vascular endothelial growth factor (Fig. 3*B*). The effect of CR-1 shedding on HUVEC migration was then evaluated with an indirect co-culture assay (Fig. 3*C*) using SW480 cells, which express little amount of CR-1 protein (Fig. 2*A*). Pretreatment of SW480 CR1 cells that were expressing an exogenous CR-1 expression vector with EGF or LPA strongly induced migration of endothelial cells, whereas these factors had significantly weaker effects on SW480 cells transfected with empty vector (SW480 EV cells) (Fig. 3*D*). These results indicate that EGF or LPA can induce endothelial cell migration toward tumor cells by inducing the release of CR-1 from tumor cells. We also tested the effect of an EGF receptor (EGFR) tyrosine kinase inhibitor, PD168393, on EGF-mediated CR-1 shedding. PD168393 dose-dependently inhibited EGF-mediated CR-1 shedding from SW480 CR1 cells at concentrations of 0.2–1.0 μM (Fig. 3*E*), which corresponds to the dose of PD168393 necessary to inhibit phosphorylation of the EGFR and of signaling molecules that are downstream of EGFR (29). PD168393 significantly suppressed the induction of endothelial cell migration by EGF-treated SW480 CR1 cells at the same range of concentrations (Fig. 3*F*), suggesting that inhibiting the EGFR may have an indirect effect for suppression of tumor angiogenesis by the ability to block CR-1 shedding from tumor cells.

Distinct Roles between Soluble and Membrane-bound Forms of CR-1—To more fully evaluate the detailed mechanism of biological activity of secreted CR-1, three artificial mutants of CR-1 in the C-terminal domain were generated: a soluble CR-1, which lacks the GPI signal (CR1ΔC Ser-161 and Ser-169), and a transmembrane CR-1 (CR1TM) in which the GPI signal was replaced by the TM domain of the EGF receptor-related receptor ErbB4, which is not cleavable by phospholipases (Fig. 4*A*). SDS-PAGE mobility of each product in the cell lysates was compatible with the estimated size from the difference in amino acid sequences (Fig. 4*B*). High amounts of both CR1ΔC mutant proteins were detected in the conditioned medium containing 1% serum, whereas a lower amount of CR1WT, and none of CR1TM, were detected (Fig. 4*C*). Immunocytochemical analysis in transiently transfected 293T cells confirmed the cell-surface localization of CR1WT and CR1TM without permeabilization following co-staining with a membrane marker wheat germ agglutinin (Fig. 4, *D* and *F*). In contrast, CR1ΔC Ser-161 (Fig. 4*E*) and Ser-169 (data not shown) mutants were undetectable without permeabilization. Intracellular trans-Golgi network localization of CR1WT, CR1ΔC Ser-161, and CR1TM was detected only after permeabilization with Triton X-100, as assessed by co-localization with a Golgi marker DsRed-Golgi (Fig. 4, *G–I*). Similar staining patterns with each mutant were obtained in transiently transfected COS7 cells (supplemental Fig. S3, *A–F*). In COS7 cells, a weak signal of extracellular deposits of CR-1 was detectable around the transfected cells in both CR1ΔC Ser-161 (data not shown) and Ser-169 (supplemental Fig. S3*B*), which was likely due to the higher amount of the overexpressed protein than that found in the CR-1-transfected 293T cells. The cell-surface expression of CR1WT and CR1TM but not soluble forms of CR-1 mutants in stably transfected 293T cells were confirmed by live cell staining with an anti-CR-1 phycoerythrin-conjugated antibody followed by FACS analysis (Fig. 4*J*).

The ability of each mutant to stimulate HUVEC migration was then assessed in an indirect co-culture migration assay with HUVECs and 293T cells that were stably transfected with empty vector or each CR-1 mutant (293T EV, CR1WT, CR1ΔC (Ser-161), (Ser-169), or CR1TM cells) (Fig. 5*A*). Under the serum-free conditions where little of the GPI-anchored CR-1 protein is released (Table 1), only 293T CR1ΔC (Ser-161 and Ser-169) cells could stimulate migration of HUVECs as compared with 293T EV cells (Fig. 5*B*). The serum-free conditioned medium from only the 293T CR1ΔC (Ser-169) cells could induce a 2- to 4-fold increase in phosphorylation of p42/44 MAPK and Akt, but not Smad2 phosphorylation in serum-starved HUVECs (Fig. 5*C*), suggesting that the effect of a soluble form of CR-1 is dependent on a Nodal-independent, MAPK/PI3K-Akt-dependent pathway as previously demonstrated (16).

To validate the biological activity of the CR-1 mutants in direct cell-to-cell interactions, a direct co-culture assay of fluorescence-labeled HUVECs with 293T transfectants was performed (Fig. 5*A*). In contrast to the indirect migration assay, when HUVECs were directly seeded onto 293T cells expressing either CR1WT, CR1TM, or CR1ΔC (Ser-169), all of the CR-1 transfectants could equally facilitate endothelial cell sprouting (Fig. 5, *D* and *E*), suggesting that cell-surface CR-1 is able to induce a response through a direct interaction with endothelial cells.

GPI-PLD Regulates CR-1 Shedding—The present results suggested that the release of CR-1 as a soluble factor may be important with respect to the ability of CR-1 to induce endothelial cell migration, leading us to delineate the mechanism(s) by which CR-1 shedding from the cell membrane might occur. We performed Triton X-114 phase partitioning to clarify whether released CR-1 is free from lipid anchoring (Fig. 6*A*). Cell-associated CR-1 was enriched in the detergent phase and not in the aqueous phase. However, PI-PLC treatment released a majority

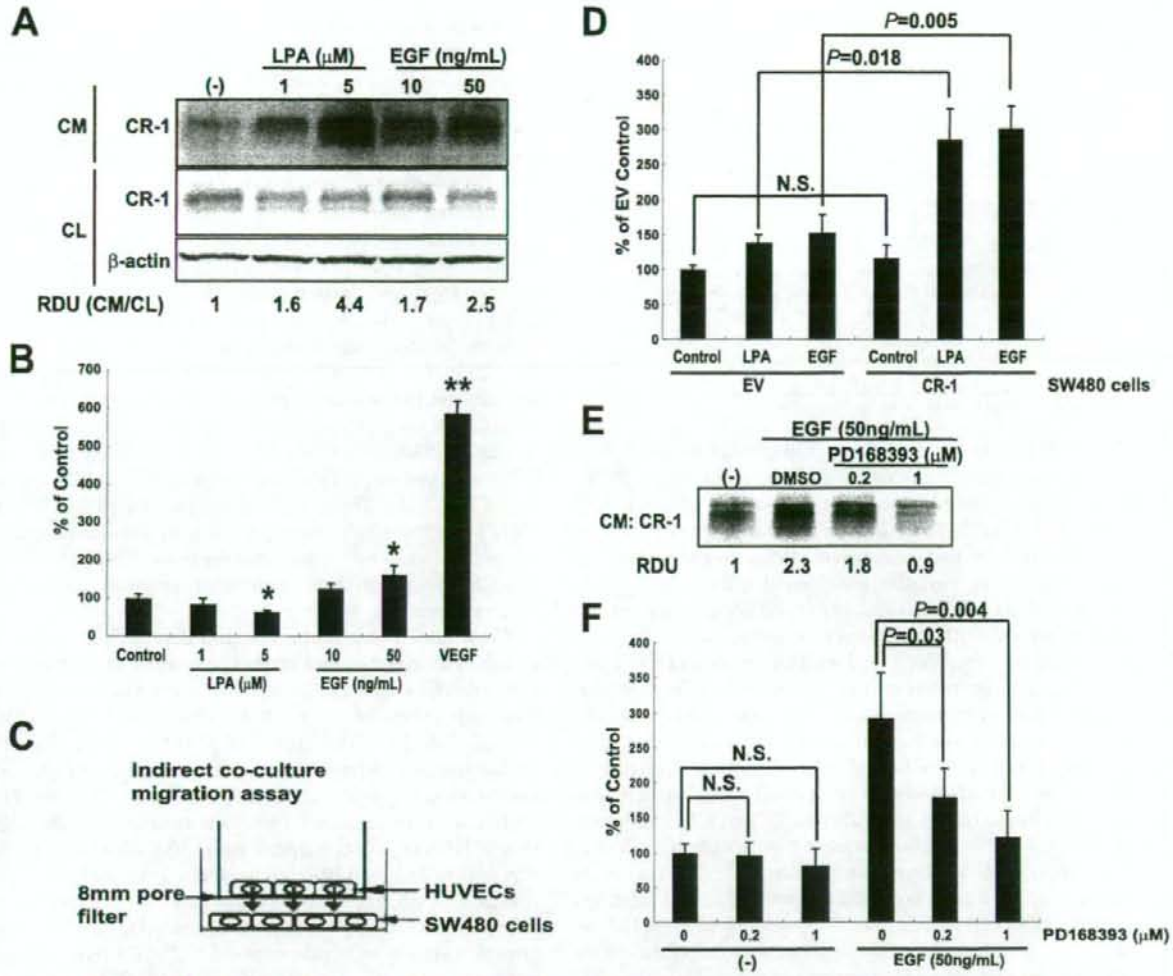

FIGURE 3. **Effects of LPA and EGF on shedding of CR-1 and endothelial cell migration.** *A*, confirmation of the effect of LPA and EGF on CR-1 shedding by Western blot analysis. SW480 CR1 cells were stimulated with the indicated factors for 6 h. *B*, direct effect of LPA and EGF on migration of HUVECs. Transwell migration assay of HUVECs was performed for the indicated factors at the indicated concentrations. Vascular endothelial growth factor (50 ng/ml) was used as a positive control. *, $p < 0.05$; **, $p < 0.01$ compared with Control. *C*, scheme of indirect co-culture migration assay. *D*, indirect effect of LPA and EGF on migration of HUVECs that are co-cultured with SW480 EV or CR1 cells. SW480 EV or CR1 cells were seeded on the bottom chamber and pretreated with indicated factors (5 μM for LPA and 50 ng/ml for EGF). After 24 h, Transwell migration assay of HUVECs was performed. *N.S.*, $p > 0.05$. *E*, effect of PD168393 on CR-1 shedding. SW480 CR1 cells were pretreated with the indicated concentrations of PD168393 for 30 min and stimulated with EGF (50 ng/ml) for 6 h. Conditioned medium was analyzed by Western blotting. *F*, effect of PD168393 on CR-1 shedding-mediated endothelial cell migration. The co-culture migration assay of HUVECs with SW480 CR1 cells was performed with the indicated concentration of PD168393 in the same condition with *D*. SW480 CR1 cells were pretreated PD168393 30 min prior to stimulation with EGF. *N.S.*, $p > 0.05$. All *graphs* represent mean ± S.D. of triplicate experiments.

of the CR-1 protein into the aqueous phase. The electrophoretic mobility of the GPI-digested form was slightly slower than the undigested form. Most of the released CR-1 in the conditioned medium was partitioned into the aqueous phase and had an electrophoretic mobility similar to PI-PLC-treated CR-1, suggesting that the released form of CR-1 shedding is free from lipid anchoring. Shedding of CR-1 may not be mediated by proteolytic digestion because increasing concentrations of serum stimulated release of CR1WT but failed to stimulate the release of CR1TM, which tethers CR-1 to the cell membrane via a transmembrane domain (Fig. 6*B*). These results may suggest that CR-1 shedding is mediated by the digestion of the GPI linkage.

GPI-PLD is involved in facilitating the shedding of a number of GPI-anchored proteins in mammalian cells (30). Serum-induced CR-1 shedding was nearly completely inhibited by the GPI-PLD inhibitor 1, 10-phenanthroline (PNT) (31) (Fig. 6*C*). In contrast, CR-1 shedding in the absence of serum was induced by 2- to 3-fold by suramin (SRM), which is reported to enhance the action of the membrane-bound GPI-phospholipases (23). RT-PCR analysis revealed that GPI-PLD mRNA is expressed in 293T, SW480, and

NTERA2/D1 cells (Fig. 6*D*). To more fully determine whether GPI-PLD is involved in directly regulating CR-1 shedding, selective knockdown experiments using human GPI-PLD-specific siRNAs (si-hGPIPLD) were undertaken. si-hGPIPLD suppressed GPI-PLD mRNA expression ~70% in 293T CR1WT cells (Fig. 6*E*), and constitutive CR-1 shed-

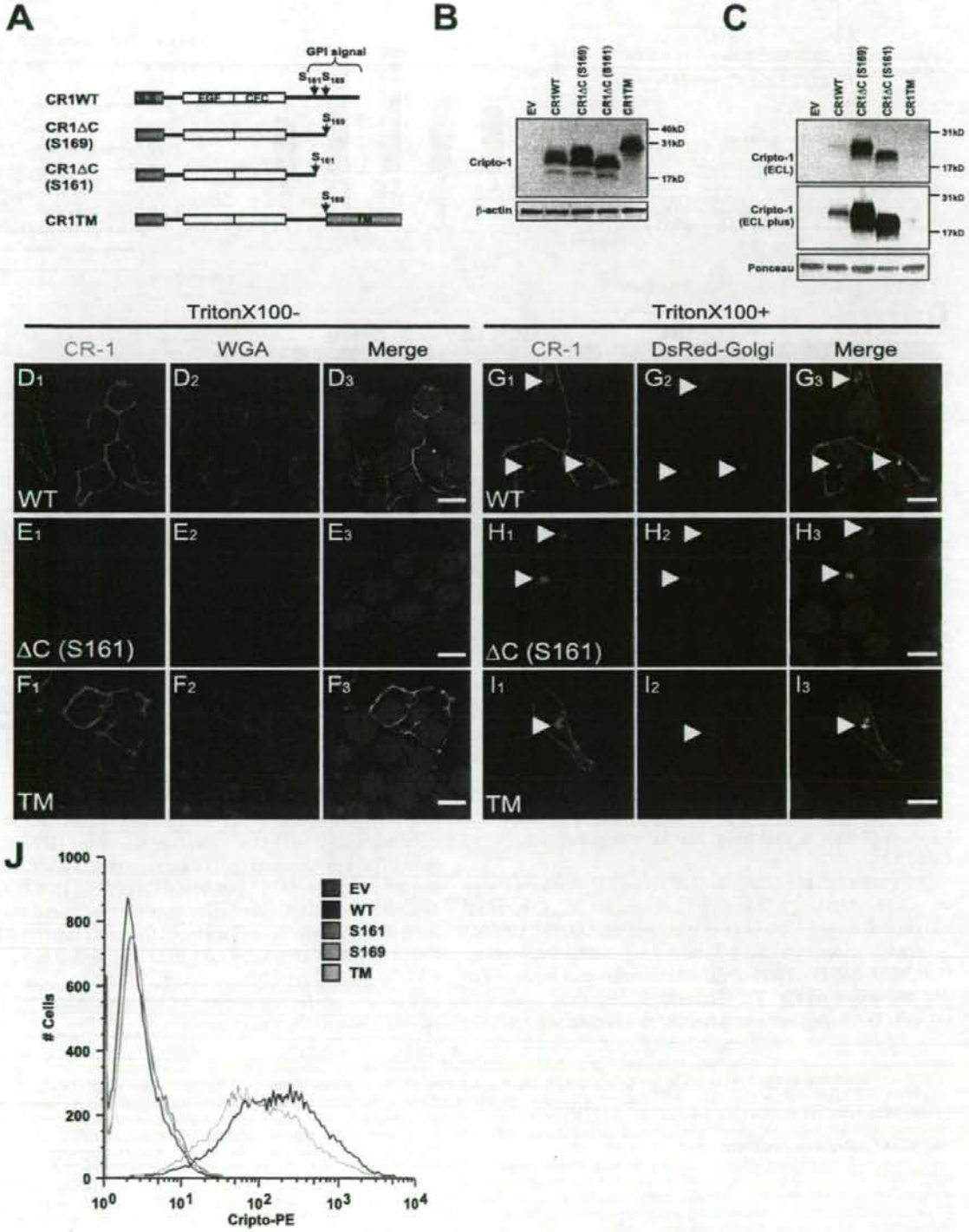

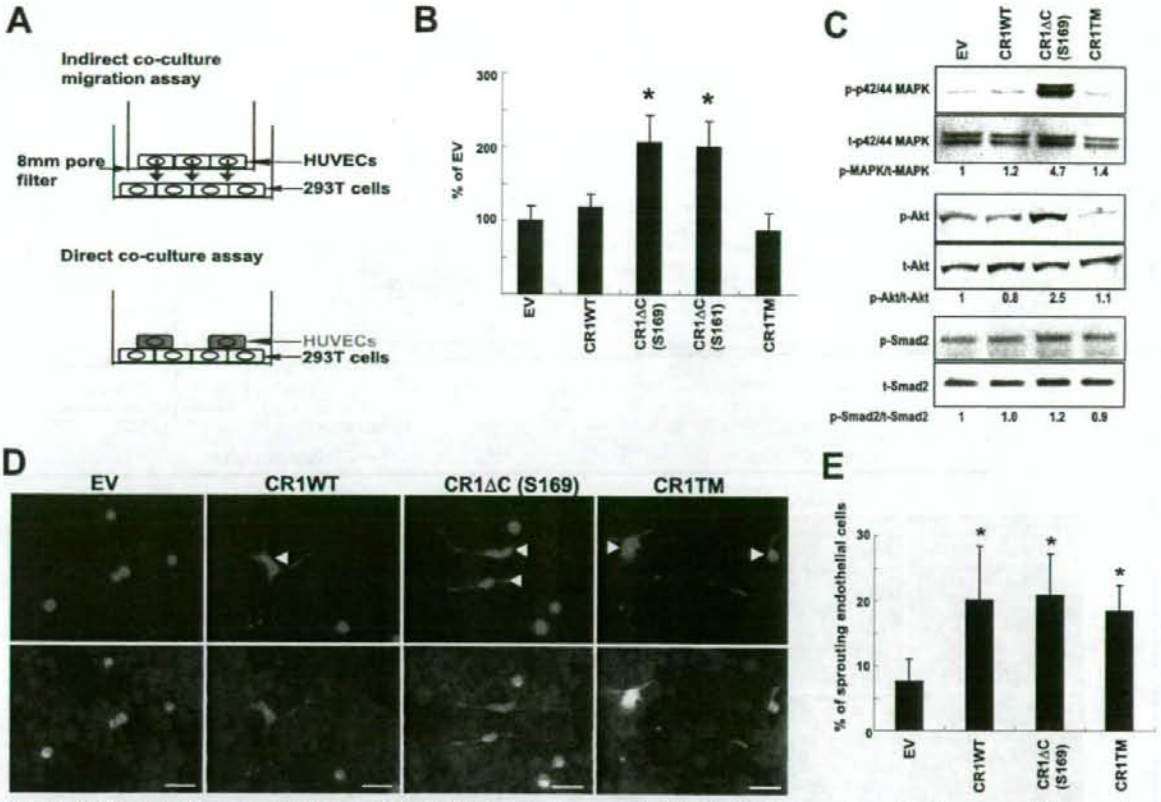

FIGURE 5. **Activity of soluble or membrane-bound forms of CR-1 mutants on endothelial cells.** *A*, indirect co-culture migration assay and direct co-culture assay (see "Experimental Procedures"). *B*, indirect co-culture migration assay using 293T cells, which had been stably transfected with the indicated expression vectors. Migration of HUVECs was evaluated. The values represent mean ± S.D. of a typical experiment performed in triplicate. *, $p < 0.05$ compared with EV. *C*, phosphorylation status of p42/44 MAPK, Akt, and Smad2 in HUVECs. HUVECs were treated with serum-free conditioned medium from 293T transfectants for 15 min. Phospho-/total protein ratio was quantified by densitometric analysis (*bottom of each panel*). *D* and *E*, direct co-culture assay using 293T cells, which had been stably transfected with indicated expression vectors. HUVECs were seeded on confluent monolayers of 293T transfectants. 5-chloromethylfluorescein diacetate labeled HUVECs (*green*) were visualized with a fluorescence microscope (*upper panels*). Counter staining was performed with F-actin (*red*) and DAPI (*blue*) (*lower panels* for three-color merged images). HUVECs with sprouting morphology (*arrowhead*) were quantified as described under "Experimental Procedures" (*E*). *Scale bar* = 50 μm. *, $p < 0.05$ compared with EV. The values represent mean ± S.D. of three independent experiments.

ding in the presence of serum was inhibited >50% after the attenuation of GPI-PLD expression (Fig. 6*F*), suggesting that CR-1 shedding is mediated by the enzymatic activity of GPI-PLD.

We then evaluated the effect of GPI-PLD overexpression on CR-1 shedding. Transient transfection of C-terminal V5-tagged mouse GPI-PLD cDNA (mGPIPLD-V5) strongly induced shedding of CR1WT into the conditioned medium from 293T cells that had been grown in serum-free medium but had little effect on CR1TM (Fig. 6*G*). A substantial amount of mGPIPLD-V5 protein was detected in conditioned medium (Fig. 6*G*), which is consistent with the previous description that GPI-PLD is a secreted enzyme (32, 33). Similar results were obtained with a wild-type (non-tagged) mouse GPI-PLD construct (data not shown). FACS analysis revealed a decrease of the cell-surface CR1WT but not of CR1TM by GPI-PLD overexpression (Fig. 6*H*), indicating that GPI-anchored CR-1 had been cleaved from the cell surface by overexpressed GPI-PLD. Overexpression of mouse GPI-PLD was also able to induce CR-1 shedding in stably transfected 293T CR1WT cells (Fig. 6*I*) and to rescue the attenuation of CR-1 shedding by siRNAs against human GPI-PLD (Fig. 6*J*).

FIGURE 4. **Generation of CR-1 mutants in the C-terminal domain.** *A*, scheme of CR-1 mutants. *B* and *C*, validation of expression of each CR-1 mutant in cell lysates and conditioned medium. 293T cells were transiently transfected with indicated expression vectors in the presence of 1% serum. Total cell lysates (*B*) and conditioned media (*C*) were collected 24 h after transfection and were analyzed by Western blot analysis. β-Actin and Ponceau S staining were used as loading controls. Results from the same blot detected by regular ECL or more sensitive ECL plus are shown in *C*. EV was used as a negative control. *D–I*, subcellular localization of CR-1 mutants. Immunocytochemistry of indicated CR-1 mutants (*green*) in transiently transfected 293T cells was performed without permeabilization (D_1–F_1) or with permeabilization by Triton X-100 (G_1–I_1). Plasma membranes were stained with wheat germ agglutinin in D_2–F_2 (*red*) and DsRed-Golgi was co-transfected with CR-1 construct in G_2–I_2. Nuclei were counterstained with DAPI (*blue*), and three-color merged images are shown in D_3–I_3. Images were visualized with confocal microscopy. *Arrowhead*, co-localization of CR-1 with Golgi marker. *Scale bar* = 20 μm. *J*, FACS analysis for the cell-surface expression of each CR-1 mutant. 293T cells stably transfected with indicated expression vectors were stained with anti-CR-1 PE-conjugated antibody and analyzed with FACS. EV was used as a negative control.

Direct physiochemical evidence of the release of CR-1 by GPI-PLD was obtained by MS analysis of secreted CR-1 in CR-1-transfected Per-C6 cells. The major GPI component of CR-1 has a structure, Ser-NH-$(CH_2)_2$-OPO_2(OH)ManManMan (phosphoethanolamine)GlcN-Hex (Fig. 7*A*). The detected mass, 3613.6 Da, for this modified peptide matches the predicted mass, 3613.49. The detected masses for all fragment ions in the MS/MS spectrum of this peptide also match the predicted ion fragments (Fig. 7*B*). The detected GPI structure of shed CR-1 is consistent with that of a protein, which is released by GPI-PLD but not by PI-PLC, because the phosphate that should be contained after PI-PLC digestion was not observed.

We then studied the role of GPI-PLD in growth factor-induced CR-1 shedding. LPA-, EGF-, and PMA-induced CR-1 shedding is also mediated by GPI-PLD, because the CR-1 shedding by these factors in SW480 CR1 cells was completely

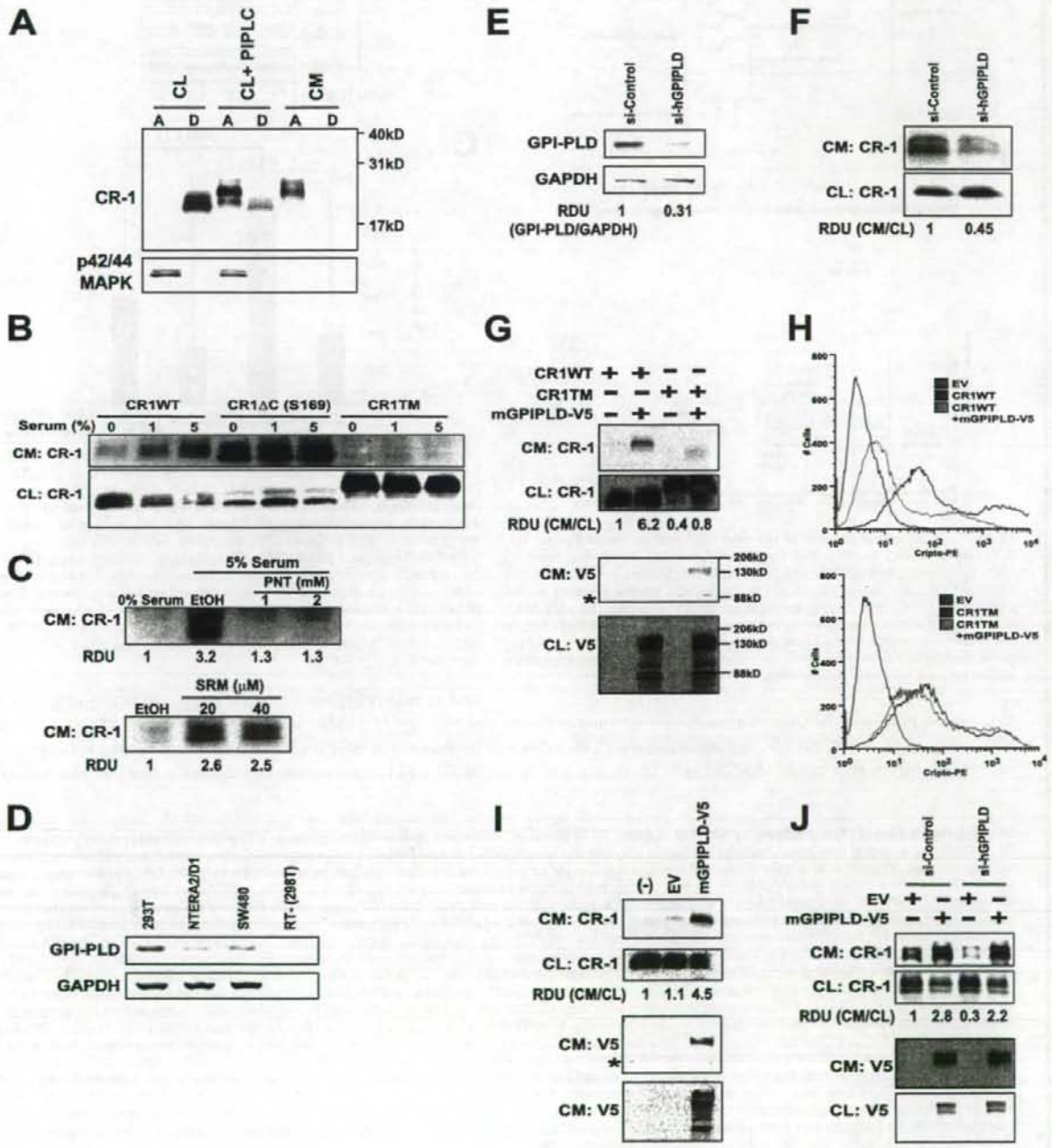

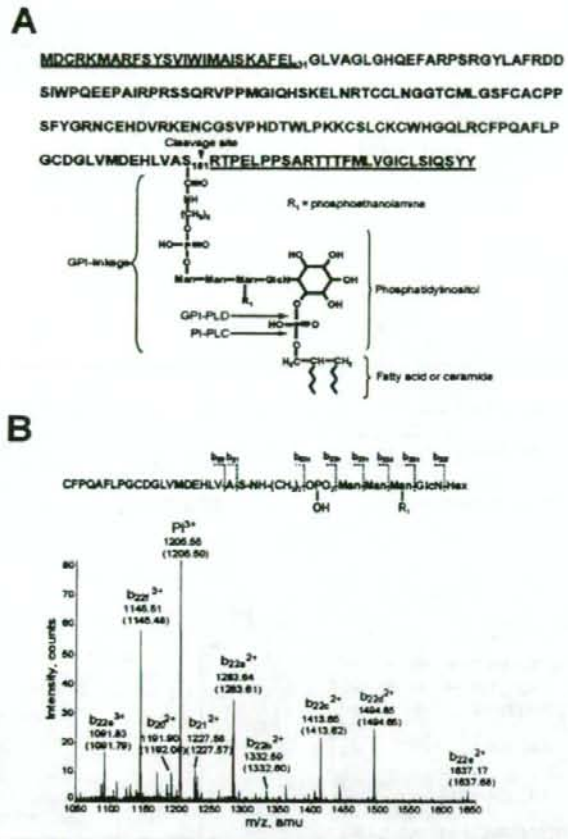

FIGURE 7. *A*, structural analysis of released CR-1 was performed using MS. *B*, enlarged MS/MS spectrum of tryptic CR-1 peptide containing residues 140–161. The sequences of the peptide, fragmentation pattern, and detected fragment ions are shown at the *top of the panel*. Cysteine residues in the peptide are pyridethylcysteine, because the protein was reduced with dithiothreitol and alkylated with 4-vinylpyridine. "*b*" designates ions that contain the N-terminal region of the peptide plus one or more amino acid residues generated by collision-induced dissociation. Calculated *m/z* values for some critical ions are shown in *parentheses*.

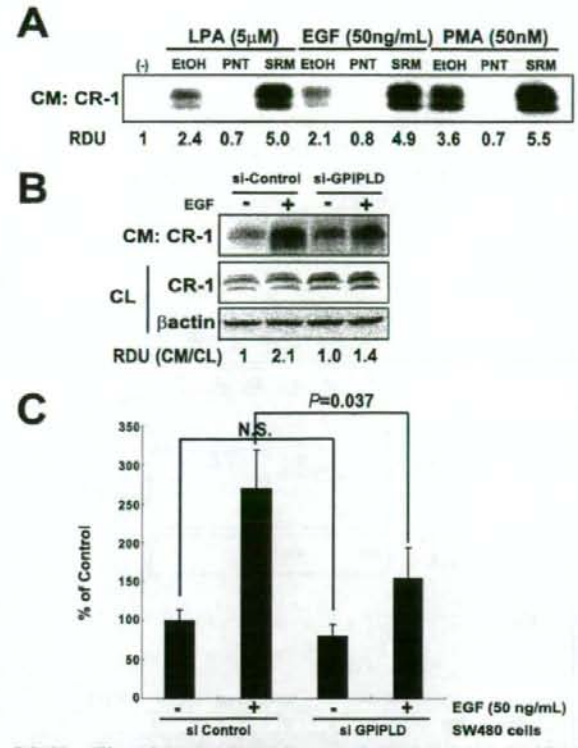

FIGURE 8. **Effect of GPI-PLD knockdown on EGF-induced CR-1 shedding and endothelial cell migration.** *A*, effect of PNT and SRM on LPA-, EGF-, or PMA-induced CR-1 shedding. SW480 CR1 cells were stimulated under indicated conditions of indicated factors for 6 h, and conditioned medium was analyzed by Western blotting. PNT, 1 mM; SRM, 20 μM. *B*, effect of GPI-PLD knockdown on EGF-induced CR-1 shedding. SW480 CR1 cells were transfected with indicated siRNAs. After 24 h, medium was replaced with serum-free medium and incubated for 16 h. Cells were then stimulated with 50 ng/ml EGF for 6 h. Released CR-1 was analyzed by Western blotting. *C*, effect of GPI-PLD knockdown on EGF-induced endothelial cell migration. SW480 CR1 cells that were treated with siRNAs as described in *B* were used for indirect co-culture migration assay with HUVECs with or without 50 ng/ml EGF stimulation. *N.S.*, $p > 0.05$.

blocked by PNT and further enhanced by combination with SRM (Fig. 8*A*). si-hGPIPLD suppressed GPI-PLD mRNA expression ~70% also in SW480 CR1 cells (data not shown), and si-hGPIPLD was able to suppress EGF-induced CR-1 shedding (2.1-fold increase in si-control and 1.4-fold increase in si-hGPIPLD, Fig. 8*B*). Furthermore, suppression of GPI-PLD expression significantly blocked the ability of

FIGURE 6. **Regulation of CR-1 shedding by GPI-PLD.** *A*, Triton X-114 phase separation was performed for cell lysates (*CL*) and conditioned medium (*CM*) from 293T CR1WT cells and analyzed by Western blotting. The same cell lysate was treated with 1 unit/ml PI-PLC. *A*, aqueous phase; *D*, detergent phase. p42/44 MAPK was used for a representative hydrophilic protein. *B*, effect of serum in shedding of each CR-1 mutant. 293T cells transfected with the indicated CR-1 mutants were incubated with 0–5% serum for 30 min, and released CR-1 in the conditioned medium was analyzed by Western blotting. *C*, effect of PNT and SRM on CR-1 shedding. Serum-starved 293T CR1WT cells were treated with or without serum for 30 min with the indicated dose of PNT (*upper panel*). The same cells were treated with the indicated dose of SRM for 30 min in the absence of serum (*lower panel*). Released CR-1 in the conditioned medium was analyzed by Western blotting. Ethanol (*EtOH*) was used for vehicle controls. *D*, GPI-PLD mRNA expression in indicated cell lines. RT-PCR was performed for 35 cycles for GPI-PLD and 25 cycles for GAPDH. The RNA from 293T cells was processed without reverse transcriptase and shown as a negative control (*RT-*). *E*, evaluation of siRNA against GPI-PLD by semi-quantitative RT-PCR. 293T cells were transfected with a total 30 nM of the indicated siRNAs, and RNA was collected 48 h after transfection. *si-Control*, mixture of three different control siRNAs; *si-GPIPLD*, mixture of three different specific siRNAs against GPI-PLD. RT-PCR was performed for 30 cycles for GPI-PLD and 20 cycles for GAPDH. *F*, effect of GPI-PLD knockdown on basal release of CR-1. 293T CR1WT cells were transfected with the indicated siRNAs. After 24 h, medium was replaced with 5% serum containing medium and incubated for 24 h. Conditioned medium was collected, and released (*CM*) and cell-associated CR-1 (*CL*) were analyzed by Western blotting. *G* and *J*, effect of V5-tagged mouse GPI-PLD (mGPIPLD-V5) overexpression on CR-1 shedding. *G*, 293T cells were transiently transfected with indicated expression vectors. After 24 h of transfection, total cell lysates (*CL*) and conditioned media (*CM*) were collected and analyzed by Western blotting. *, nonspecific bands. *H*, 293T cells were transiently transfected with the indicated expression vectors. After 24 h of transfection, cell-surface CR-1 was stained with anti-CR-1 PE-conjugated antibody and analyzed by FACS. *I*, stably transfected 293T CR1WT cells were transfected with indicated expression vectors. EV was used as a negative control and non-transfected control is also shown (−). After 24 h, total cell lysates (*CL*) and conditioned media (*CM*) were collected and analyzed by Western blotting. *J*, 293T CR1WT cells were co-transfected with the indicated siRNAs and expression vectors. After 24 h, medium was replaced with 5% serum containing medium and incubated for 24 h. Total cell lysates (*CL*) and conditioned medium (*CM*) were collected and analyzed by Western blotting.

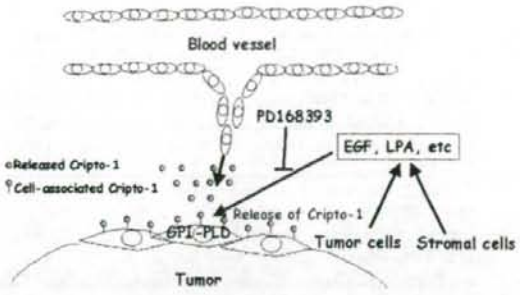

FIGURE 9. **Mechanism of CR-1-mediated tumor angiogenesis.**

SW480 CR1 cells to induce endothelial cell migration upon EGF stimulation (Fig. 8*C*).

DISCUSSION

We have previously shown that CR-1 exhibits pro-angiogenic activity through a Nodal-independent, c-Src/MAPK/PI3K-Akt-dependent pathway (16). In the present study, we have further delineated the mechanism by which CR-1 can function as an endothelial migration factor. Soluble forms of CR-1 protein were able to induce endothelial migration in contrast to the cell-associated CR-1. On the other hand, membrane-bound forms (a GPI-anchored or a transmembrane form) of CR-1 were able to induce endothelial cell sprouting through a direct cell-to-cell interaction. These findings suggest that soluble CR-1 can act as a paracrine chemoattractant for endothelial cells and that membrane-bound CR-1, which is expressed on the surface of tumor cells, can locally stimulate endothelial cells to potentially form vessels.

Previous reports have shown that the shedding of GPI-anchored proteins can be induced by various factors (34), some of which were also found to facilitate CR-1 shedding in colon cancer cells, such as PMA (35) and EGF (36). The present study demonstrates that LPA or EGF can stimulate tumor cells that are expressing CR-1 to facilitate shedding, which could then possibly enhance endothelial cell migration. The concentration of CR-1 protein from SW480 cells stimulated with growth factors such as EGF or LPA was ~40–60 ng/ml by enzyme-linked immunosorbent assay, and we have previously reported that the range plasma CR-1 level in the clinical cancer patients was 0.86–19.18 ng/ml. Based on these findings, it is speculated that the local concentration of CR-1 protein in clinical tumor tissues could be high enough for its biological activity. The present findings may also explain one additional indirect mechanism by which either LPA or EGF might induce tumor angiogenesis (27, 28). The fact that an EGFR inhibitor blocked the effect of EGF to facilitate CR-1 shedding and subsequently to attract endothelial cells may suggest the possible usage of EGFR inhibitors to block tumor angiogenesis enhanced by CR-1 shedding (Fig. 9).

This is the first study to define a detailed cellular mechanism by which CR-1 can be released as a soluble growth factor. Native or overexpressed CR-1 protein was released from cells into the conditioned medium by stimuli, such as serum, PMA, or several growth factors or cytokines. Release of GPI-anchored CR-1 was found to be mediated by GPI-PLD, which is the only identified mammalian phospholipase that can cleave the GPI linkage of GPI-anchored proteins (30). Recent reports have shown that the tumor marker carcinoembryonic antigen, which is also a GPI-anchored protein, is released from cells by the enzymatic activity of GPI-PLD in a regulatory mechanism that is similar to the release of CR-1 (37, 38). In addition, CR-1 was found to be present in the plasma of breast and colon cancer patients, suggesting the possible use of plasma CR-1 levels as a tumor marker (20). Therefore, the regulation of CR-1 shedding might also be important for diagnosis of cancer.

CR-1 shedding by GPI-PLD is inducible by certain stimuli such as serum, EGF, or LPA. A PLCγ-PKC intracellular signaling pathway is known to be a common signaling pathway that is activated by these factors (39, 40). In fact, the PLCγ inhibitor or the PKC inhibitor blocked CR-1 shedding induced by these factors. These data suggest inducible regulation of the enzymatic activity of GPI-PLD via a PLCγ-PKC pathway, although there are no reports of such inducible activation of this enzyme. To prove the inducible activation of this enzyme, analysis based on enzyme assay(s) should be performed in the future. Because GPI-PLD is a secreted enzyme as described previously (33) and as we demonstrated here, the translocation of CR-1 protein could be another possible mechanism of inducible shedding of CR-1 by GPI-PLD.

The importance of ectodomain shedding of cell-associated pro-ligands has previously been described (41). In this context, the EGF family of growth factors are initially synthesized as membrane-bound precursors and processed by a disintegrin and metalloproteinase domain (ADAM) proteases to function as mature ligands (42, 43). Inhibition of shedding of EGF-related growth factors may be effective as a therapeutic target of cancer (44). Initially, CR-1 was discovered as an EGF-related peptide and has since been shown to induce signaling through a Nodal-independent signaling pathway that is similar to pathways that are activated by EGF family ligands through the EGFR (1, 3). Even though the one or more precise mechanisms of this Nodal-independent signaling pathway, including its receptor(s) or functional domain(s), remain to be investigated, it is likely that the shedding of CR-1 might have similar importance with that of other EGF family ligands. This study strongly suggests the possibility that the angiogenic and oncogenic effects of CR-1 might be enhanced by its shedding and that shedding of CR-1 could be a potential target for cancer therapy.

Acknowledgments—We are grateful to Brenda W. Jones for providing technical support, to Susan Garfield and Stephen Wincovitch for help in confocal imaging, and to the National Institutes of Health Fellows Editorial Board for assistance with editing.

REFERENCES

1. Salomon, D. S., Bianco, C., Ebert, A. D., Khan, N. I., De Santis, M., Normanno, N., Wechselberger, C., Seno, M., Williams, K., Sanicola, M., Foley, S., Gullick, W. J., and Persico, G. (2000) *Endocr. Relat. Cancer* **7**, 199–226
2. Shen, M. M. (2007) *Development* **134**, 1023–1034
3. Bianco, C., Strizzi, L., Normanno, N., Khan, N., and Salomon, D. S. (2005) *Curr. Top. Dev. Biol.* **67**, 85–133
4. Xing, P. X., Hu, X. F., Pietersz, G. A., Hosick, H. L., and McKenzie, I. F.

(2004) *Cancer Res.* **64,** 4018–4023
5. Strizzi, L., Bianco, C., Normanno, N., Seno, M., Wechselberger, C., Wallace-Jones, B., Khan, N. I., Hirota, M., Sun, Y., Sanicola, M., and Salomon, D. S. (2004) *J. Cell. Physiol.* **201,** 266–276
6. Wechselberger, C., Strizzi, L., Kenney, N., Hirota, M., Sun, Y., Ebert, A., Orozco, O., Bianco, C., Khan, N. I., Wallace-Jones, B., Normanno, N., Adkins, H., Sanicola, M., and Salomon, D. S. (2005) *Oncogene* **24,** 4094–4105
7. Sun, Y., Strizzi, L., Raafat, A., Hirota, M., Bianco, C., Feigenbaum, L., Kenney, N., Wechselberger, C., Callahan, R., and Salomon, D. S. (2005) *Am. J. Pathol.* **167,** 585–597
8. Adkins, H. B., Bianco, C., Schiffer, S. G., Rayhorn, P., Zafari, M., Cheung, A. E., Orozco, O., Olson, D., De Luca, A., Chen, L. L., Miatkowski, K., Benjamin, C., Normanno, N., Williams, K. P., Jarpe, M., LePage, D., Salomon, D., and Sanicola, M. (2003) *J. Clin. Invest.* **112,** 575–587
9. De Luca, A., Arra, C., D'Antonio, A., Casamassimi, A., Losito, S., Ferraro, P., Ciardiello, F., Salomon, D. S., and Normanno, N. (2000) *Oncogene* **19,** 5863–5871
10. Yeo, C., and Whitman, M. (2001) *Mol. Cell* **7,** 949–957
11. Cheng, S. K., Olale, F., Bennett, J. T., Brivanlou, A. H., and Schier, A. F. (2003) *Genes Dev.* **17,** 31–36
12. Chen, C., Ware, S. M., Sato, A., Houston-Hawkins, D. E., Habas, R., Matzuk, M. M., Shen, M. M., and Brown, C. W. (2006) *Development* **133,** 319–329
13. Bianco, C., Adkins, H. B., Wechselberger, C., Seno, M., Normanno, N., De Luca, A., Sun, Y., Khan, N., Kenney, N., Ebert, A., Williams, K. P., Sanicola, M., and Salomon, D. S. (2002) *Mol. Cell. Biol.* **22,** 2586–2597
14. Gray, P. C., Shani, G., Aung, K., Kelber, J., and Vale, W. (2006) *Mol. Cell. Biol.* **26,** 9268–9278
15. Ding, J., Yang, L., Yan, Y. T., Chen, A., Desai, N., Wynshaw-Boris, A., and Shen, M. M. (1998) *Nature* **395,** 702–707
16. Bianco, C., Strizzi, L., Ebert, A., Chang, C., Rehman, A., Normanno, N., Guedez, L., Salloum, R., Ginsburg, E., Sun, Y., Khan, N., Hirota, M., Wallace-Jones, B., Wechselberger, C., Vonderhaar, B. K., Tosato, G., Stetler-Stevenson, W. G., Sanicola, M., and Salomon, D. S. (2005) *J. Natl. Cancer Inst.* **97,** 132–141
17. Minchiotti, G., Parisi, S., Liguori, G., Signore, M., Lania, G., Adamson, E. D., Lago, C. T., and Persico, M. G. (2000) *Mech. Dev.* **90,** 133–142
18. Minchiotti, G., Manco, G., Parisi, S., Lago, C. T., Rosa, F., and Persico, M. G. (2001) *Development* **128,** 4501–4510
19. Yan, Y. T., Liu, J. J., Luo, Y. E. C., Haltiwanger, R. S., Abate-Shen, C., and Shen, M. M. (2002) *Mol. Cell. Biol.* **22,** 4439–4449
20. Bianco, C., Strizzi, L., Mancino, M., Rehman, A., Hamada, S., Watanabe, K., De Luca, A., Jones, B., Balogh, G., Russo, J., Mailo, D., Palaia, R., D'Aiuto, G., Botti, G., Perrone, F., Salomon, D. S., and Normanno, N. (2006) *Clin. Cancer Res.* **12,** 5158–5164
21. Watanabe, K., Hasegawa, Y., Yamashita, H., Shimizu, K., Ding, Y., Abe, M., Ohta, H., Imagawa, K., Hojo, K., Maki, H., Sonoda, H., and Sato, Y. (2004) *J. Clin. Invest.* **114,** 898–907
22. McCabe, J. B., and Berthiaume, L. G. (2001) *Mol. Biol. Cell* **12,** 3601–3617
23. Lee, J. Y., Kim, M. R., and Sok, D. E. (1998) *Neurochem. Res.* **23,** 899–905
24. Jacobson, K., Mouritsen, O. G., and Anderson, R. G. (2007) *Nat. Cell Biol.* **9,** 7–14
25. Muller, H. K., Wiborg, O., and Haase, J. (2006) *J. Biol. Chem.* **281,** 28901–28909
26. Paladino, S., Pocard, T., Catino, M. A., and Zurzolo, C. (2006) *J. Cell Biol.* **172,** 1023–1034
27. van Cruijsen, H., Giaccone, G., and Hoekman, K. (2005) *Int. J. Cancer* **117,** 883–888
28. Sengupta, S., Wang, Z., Tipps, R., and Xu, Y. (2004) *Semin. Cell Dev. Biol.* **15,** 503–512
29. Bose, R., Molina, H., Patterson, A. S., Bitok, J. K., Periaswamy, B., Bader, J. S., Pandey, A., and Cole, P. A. (2006) *Proc. Natl. Acad. Sci. U. S. A.* **103,** 9773–9778
30. Lauc, G., and Heffer-Lauc, M. (2006) *Biochim. Biophys. Acta* **1760,** 584–602
31. Metz, C. N., Brunner, G., Choi-Muira, N. H., Nguyen, H., Gabrilove, J., Caras, I. W., Altszuler, N., Rifkin, D. B., Wilson, E. L., and Davitz, M. A. (1994) *EMBO J.* **13,** 1741–1751
32. Ikezawa, H. (2002) *Biol. Pharm. Bull.* **25,** 409–417
33. Kung, M., Butikofer, P., Brodbeck, U., and Stadelmann, B. (1997) *Biochim. Biophys. Acta* **1357,** 329–338
34. Sharom, F. J., and Lehto, M. T. (2002) *Biochem. Cell Biol.* **80,** 535–549
35. Parkin, E. T., Watt, N. T., Turner, A. J., and Hooper, N. M. (2004) *J. Biol. Chem.* **279,** 11170–11178
36. Roberts, J. M., Kenton, P., and Johnson, P. M. (1990) *FEBS Lett.* **267,** 213–216
37. Yamamoto, Y., Hirakawa, E., Mori, S., Hamada, Y., Kawaguchi, N., and Matsuura, N. (2005) *Biochem. Biophys. Res. Commun.* **333,** 223–229
38. Naghibalhossaini, F., and Ebadi, P. (2006) *Cancer Lett.* **234,** 158–167
39. Carpenter, G., and Ji, Q. (1999) *Exp. Cell Res.* **253,** 15–24
40. Newton, A. C. (2001) *Chem. Rev.* **101,** 2353–2364
41. Arribas, J., and Borroto, A. (2002) *Chem. Rev.* **102,** 4627–4638
42. Normanno, N., Bianco, C., De Luca, A., and Salomon, D. S. (2001) *Front. Biosci.* **6,** D685–D707
43. Zhou, B. B., Peyton, M., He, B., Liu, C., Girard, L., Caudler, E., Lo, Y., Baribaud, F., Mikami, I., Reguart, N., Yang, G., Li, Y., Yao, W., Vaddi, K., Gazdar, A. F., Friedman, S. M., Jablons, D. M., Newton, R. C., Fridman, J. S., Minna, J. D., and Scherle, P. A. (2006) *Cancer Cell* **10,** 39–50
44. Singh, A. B., and Harris, R. C. (2005) *Cell. Signal.* **17,** 1183–1193

REGULAR PAPER

J. Physiol. Sci. Vol. 57, No. 4; Aug. 2007; pp. 235–239
Online Sep. 15, 2007; **doi:10.2170/physiolsci.RP006607**

A Cdk5 Inhibitor Enhances the Induction of Insulin Secretion by Exendin-4 Both in Vitro and in Vivo

Kohsuke KITANI[1], Shigeo OGUMA[1], Tei-ichi NISHIKI[1], Iori OHMORI[1], Hervé GALONS[2], Hideki MATSUI[1], Laurent MEIJER[3], and Kazuhito TOMIZAWA[1]

[1]Department of Physiology, Okayama University Graduate School of Medicine, Dentistry, and Pharmaceutical Sciences, Okayama, 700-8558 Japan; [2]Université René Descartes, 4, Avenue de l'Observatoire, 75006 Paris, France; and [3]Amyloids and Cell Division Cycle, Station Biologique de Roscoff, CNRS, Place Georges Teissier, Roscoff 29680, France

Abstract: Exendin-4 (Ex4) is a peptide found in the lizard *Heloderma suspectum*, and it has a high similarity to glucagon-like peptide 1 (GLP-1). It induces insulin secretion without the risk of hypoglycemic episodes. Cyclin-dependent kinase 5 (Cdk5) is a serine/threonine kinase that is predominantly expressed in neurons. Recent studies have shown that this kinase regulates glucose-stimulated insulin secretion. Cdk5 inhibition enhances insulin secretion under conditions of stimulation by high glucose, but not low glucose. In the present study, we examined whether R-roscovitine (R-ros), a Cdk5 inhibitor, enhances insulin secretion induced by Ex4. R-ros induced Ex4-dependent insulin secretion under conditions of high glucose, but not low glucose in MIN6B1 cells. The enhancement by R-ros was also observed in *db/db* mice, a mouse model of type 2 diabetes. Moreover, long-term treatment with Ex4 and R-ros significantly improved HbA1c compared with treatment using only Ex4. These results suggest that a co-application of R-ros and Ex4 may become a promising therapy for the treatment of type 2 diabetes.

Key words: Cdk5, signal transduction, GLP-1, insulin secretion, beta cell.

The onset of type 2 diabetes is marked by a selective loss of pancreatic beta cells and insulin secretory dysfunction; thus, insulin production and secretion no longer compensate for inherent insulin resistance [1, 2]. One therapeutic approach for type 2 diabetes has been to use pharmacological reagents that increase endogenous insulin secretion, such as sulfonylurea and GLP-1 analogues [3, 4]. Sulfonylurea induces insulin secretion by blocking ATP-sensitive K^+ channels. This in turn causes beta cell plasma membrane depolarization and a consequent opening of the L-type voltage-dependent Ca^{2+} channels (L-VDCCs) [5]. The rise in cytosolic $[Ca^{2+}]_i$ triggers insulin exocytosis [6, 7]. However, sulfonylurea has the shortcoming of inducing insulin secretion independently of the circulating glucose concentration, and this increases the risk of the incidence of hypoglycemic episodes [3].

Exendin-4 (Ex4) is a GLP-1 analogue and mimics the action of endogenous GLP-1 [8]. GLP-1 acts physiologically on beta cells via specific Gαs-protein-coupled GLP-1 receptors to potentiate glucose-induced insulin secretion [9]. Endogenous GLP-1 has a short half-life of ~2 min in vivo because of proteolysis by a protease, dipeptidyl peptidase IV (DPP-IV) [10]. Ex4 is relatively resistant to DPP-IV proteolysis and consequently has a longer half-life in the circulation than native GLP-1 [11]. Ex4 promotes insulin secretion in a glucose-dependent manner [8]. Therefore, the risk of hypoglycemia is lessened when Ex4 is used therapeutically. The major molecular mechanism of the induction of insulin secretion by Ex4 is thought to be the potentiation of glucose-stimulated proinsulin biosynthesis at the translational level, and a mobilization of insulin secretory vesicles into a readily releasable pool through the activation of PKA [12]. Moreover, Ex4 potentiates L-type voltage-dependent calcium channel (L-VDCC) current via the PKA pathway [13].

Cdk5 is predominantly expressed in neurons and regulates neural functions such as neural development, synaptic plasticity, and neurotransmission [14]. It had been thought for a long time that Cdk5 functions only in neurons. However, recent studies have shown that a high level of Cdk5 activity is also observed in beta cells, and Cdk5 regulates insulin secretion [15, 16]. The inhibition of Cdk5 by selective inhibitors such as olomoucine and R-ros increases insulin secretion in beta cells in a glucose-dependent manner [15]. The mechanism of the induction of insulin secretion by Cdk5 inhibitors has been shown to be as follows: insulin secretion is triggered by calcium influx through L-type voltage-dependent calcium channels

Received on Jun 18, 2007; accepted on Sep 13, 2007; released online on Sep 15, 2007; doi:10.2170/physiolsci.RP006607
Correspondence should be addressed to: Kazuhito Tomizawa, Department of Physiology, Okayama University Graduate School of Medicine, Dentistry and Pharmaceutical Sciences, Shikata-cho 2-5-1, Okayama, 700-8558 Japan. Tel: +81-86 235-7109, Fax: +81-86 235-7111, E-mail: tomikt@md.okayama-u.ac.jp

(L-VDCCs) in response to an elevation of the extracellular glucose level. Cdk5 phosphorylates loop II-III of the α1c subunit of L-VDCC and inhibits the channel activity, resulting in the inhibition of glucose-stimulated insulin secretion [15]. Cdk5 inhibitors increase Ca^{2+} influx through L-VDCC after plasma membrane depolarization, but not under conditions of low glucose.

Thus, both Ex4 and R-ros enhance insulin secretion in a glucose-dependent manner by a part but not all of the different mechanisms in beta cells. These results suggest that co-treatment with the two drugs might induce more insulin secretion compared with treatment with each drug alone without the risk of hypoglycemia. In the present study, we examined the effect of co-treatment with Ex4 and R-ros on insulin secretion both in vitro and in *db/db* mice, an animal model of type 2 diabetes.

METHODS

Cell line. MIN6 B1 (MIN6B1) cells were a gift from Dr. J.C. Irminger (University of Geneva, Switzerland). The cells were cultured in DMEM with 15% fetal calf serum, 25 mM glucose, 71 mM 2-mercaptoethanol, and 2 mM glutamine until use.

Animals. Male C57BL/KsOlaHsd-Lepr (*db/db*) mice were obtained from Jackson Laboratories (Bar Harbor, ME, USA). The animals were housed 2–3 per cage at 24°C with a 12 h light/dark cycle and were acclimated for at least 6 days before use. Food and water were provided ad libitum.

Measurement of insulin secretion in MIN6 cells. Insulin secretion in MIN6 cells was measured as described previously [15]. Briefly, MIN6 cells (0.4×10^6) were seeded into 24-well dishes (Asahi Techno Glass, Tokyo, Japan) for 48 h before use. The cells were then incubated for 2 h in KRB containing 2.8 mM glucose, followed by KRB with 50 μM R-ros [17] and/or 5 nM Ex4 (Sigma-Aldrich, St. Louis, MO) for 1 h. The cells were then stimulated with low (2.8 mM) or high (16.7 mM) glucose in the presence or absence of R-ros and Ex4 for 1 h. The culture medium was then collected and used for the measurement of insulin concentration. The concentration was determined by a radio-immuno assay (Eiken Chemical, Tokyo, Japan), applied according to the manufacturer's protocol.

Intraperitoneal glucose tolerance test and measurement of plasma insulin level. The glucose tolerance test was performed as described previously [15]. Briefly, 6-week-old or 32-week-old *db/db* mice were subjected to fasting for 17 h. They were then subcutaneously injected with 100 μg/kg Ex4 and various concentrations of R-ros. As a control, the mice were injected with DMSO. After 1 h, they were intraperitoneally injected with glucose (1 g/kg). Blood samples were collected before and 15, 20, 30, and 60 min after the administration of glucose. Glucose levels were measured using a glucometer (GR-102, Terumo, Tokyo, Japan).

For the analysis of plasma insulin in 6-week-old *db/db* mice, blood samples were collected 30 min after the administration of glucose. The plasma was prepared by the addition of heparin and subsequent centrifugation at 16,000 rpm for 15 min. Insulin concentration was measured by an ELISA method according to the manufacturer's protocol (Ultrasensitive rat insulin ELISA kit, Crystal Chem, Chicago, IL, USA).

Long-term treatment with R-ros and Exendin-4 and measurement of HbA1c. Six-week-old *db/db* mice were injected subcutaneously with Ex4 (100 μg/kg) and/or R-ros (7 mg/kg) twice a day for 40 consecutive days. The mice were then sacrificed and their blood collected. HbA1c levels were assessed using a DCA2000 (Bayer Diagnostics, Tarrytown, NY, USA), a portable device that employs a monoclonal antibody directed against part of the sequence of the HbA1c molecule.

Statistics. Values are reported as the mean ± SD. Data were analyzed using Student's *t*-test to compare two conditions, and one-way ANOVA was followed by Scheffe's post-hoc analysis to compare multiple conditions. $P < 0.05$ was considered to be significant.

RESULTS

1. Effect of cotreatment with Ex4 and R-ros on insulin secretion from MIN6B1 cells

MIN6B1 cells were established as a subline derived from the mouse pancreatic beta-cell line MIN6, and they respond to glucose in a concentration- and cell-confluence–dependent manner [18]. Ex4 did not affect insulin secretion from MIN6B1 cells under conditions of low glucose stimulation (Fig. 1A). The co-application of Ex4 and R-ros also had no effect on the insulin secretion under conditions of low glucose (Fig. 1A). In contrast, Ex4 significantly induced insulin secretion when stimulated with high glucose (Fig. 1B). Moreover, R-ros enhanced Ex4-induced insulin secretion under conditions of high glucose (Fig. 1B).

2. Effects of Ex4 and R-ros on blood glucose level in *db/db* mice

To investigate whether a co-application of Ex4 and R-ros decreases the blood glucose level in a model of type 2 diabetes, we examined the effect of these drugs on the blood glucose level by performing intraperitoneal glucose-tolerance tests on *db/db* mice; they have an inactivating mutation in the leptin receptor gene, resulting in a shorter intracellular domain of the receptor that is unable to transduce signals [19]. Their phenotype consists of obesity, insulin resistance, and diabetes, similar to type 2 diabetes in humans [20]. In control mice, the blood glucose

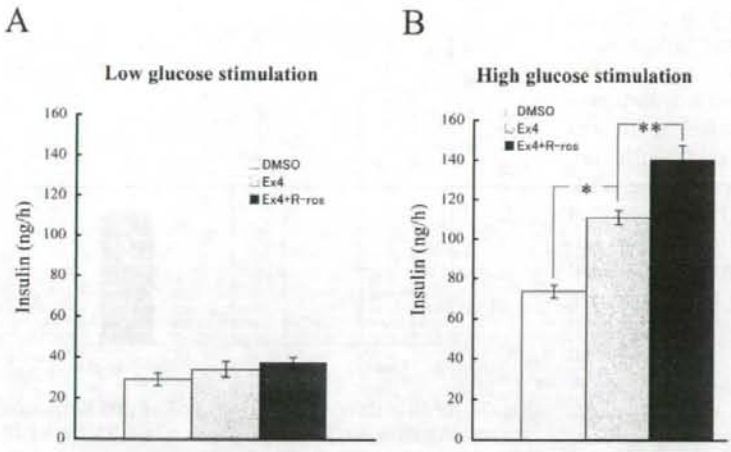

Fig. 1. Effect of Ex4 and R-ros on insulin secretion from MIN6B1 cells. The cells were stimulated with (**A**) low glucose (2.8 mM) or (**B**) high glucose (16.7 mM). $n = 6$ each group. $^{*}P < 0.005$ versus (v.s.) control, $^{**}P < 0.01$ v.s. control.

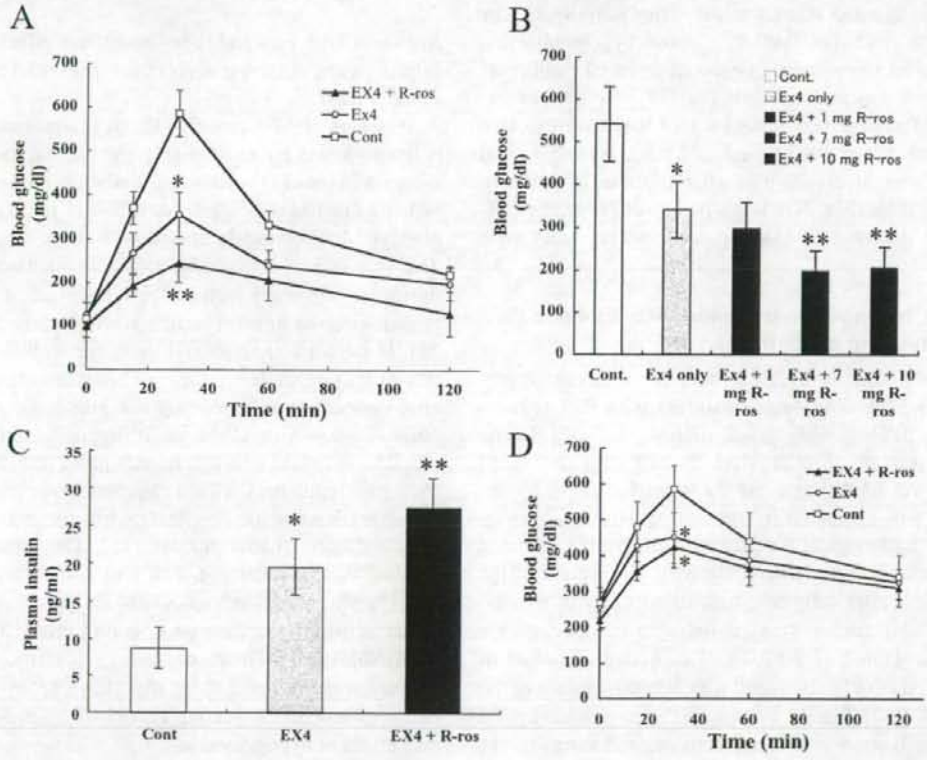

Fig. 2. Intraperitoneal glucose-tolerance test in *db/db* mice. **A**: Comparison of blood glucose levels after glucose injection in *db/db* mice treated with Ex4 alone or with a combination of Ex4 and R-ros. The mice were treated with 100 μg/kg Ex4 and/or 7 mg/kg R-ros. $n = 8$ each group. $^{*}P < 0.01$ v.s. control, $^{**}P < 0.01$ v.s. Ex4 only. **B**: Effect of various concentrations of R-ros on Ex4-dependent reduction of blood glucose level 30 min after glucose injection. $n = 8$ each group. $^{*}P < 0.01$ v.s. control, $^{**}P < 0.01$ v.s. Ex4 alone. **C**: Effect of R-ros on Ex4-induced plasma insulin level in *db/db* mice. The mice were treated with 100 μg/kg Ex4 and/or 10 mg/kg R-ros 1 h before the administration of glucose. $n = 6$ each group. $^{*}P < 0.005$ v.s. control, $^{**}P < 0.01$ v.s. Ex4 alone. **D**: Effect of Ex4 and R-ros on blood glucose level in 32-week-old mice. $n = 9$–10 each group. $^{*}P < 0.05$ v.s. control.

level 30 min after glucose injection increased and was close to 600 mg/dl (Fig. 2A). Ex4 administration inhibited the blood glucose level increase 30 min after glucose injection (Fig. 2, A and B). The co-administration of Ex4

and R-ros (7 mg/kg) was more effective in inhibiting the increase in blood glucose level 30 min after glucose injection than the administration of Ex4 alone (Fig. 2A). The dose-dependency of the effect of R-ros on the reduction of the blood glucose level by Ex4 was examined. A low concentration (1 mg/kg) of R-ros did not affect the inhibitory effect of Ex4 on blood glucose level 30 min after glucose injection (Fig. 2B). In contrast, the blood glucose level in the mice co-treated with 7 or 10 mg/kg R-ros and Ex4 significantly decreased compared with that in mice treated with Ex4 alone (Fig. 2B). In agreement with the results, 10 mg/kg R-ros further induced the plasma insulin level compared with that of Ex4 alone (Fig. 2C). Ex4 enhanced the plasma insulin level 30 min after glucose application, and the co-application of Ex4 and R-ros was more effective in the induction of the plasma insulin level (Fig. 2C).

db/db mice exhibit biphasic changes of glucose metabolism in an age-dependent manner. They initially display hyperinsulinemia, but later they show hypoinsulinemia because of an impairment of glucose-induced insulin secretion from pancreatic β-cells [21, 22]. We next examined the effect of the co-application of R-ros with Ex4 on blood glucose levels in 32-week-old mice. Ex4 decreased blood glucose levels 30 min after glucose injection in these older mice (Fig. 2D). R-ros had no effect on the Ex4-dependent decrease of blood glucose level in the mice (Fig. 2D)

3. Effects of long-term treatment with Ex4 and R-ros on HbA1c in *db/db* mice

Clinical studies have shown that Ex4 improves hyperglycemia and that long-term treatment with Ex4 reduces HbA1c in patients with type 2 diabetes [23–25]. In the present study, *db/db* mice were treated with Ex4 with/without R-ros for 40 days, and the improvement of hyperglycemia was evaluated by measuring HbA1c. We observed no pathological disorders in *db/db* mice injected with 7 mg/kg R-ros (data not shown). The weight of the mice 40 days after daily administrations of R-ros was the same as that in control mice (R-ros-injected mice, 46.4 ± 3.5 g; control mice, 47.2 ± 3.2 g). Daily administrations of Ex4 reduced HbA1c compared with administrations of the control (DMSO) (Fig. 3). Moreover, the co-administration of Ex4 and R-ros was more effective in reducing HbA1c than the administration of Ex4 alone (Fig. 3).

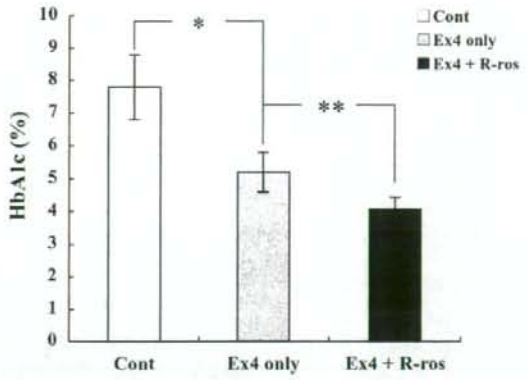

Fig. 3. HbA1c in *db/db* mice treated with Ex4 and R-ros for 40 consecutive days. $n = 9–10$ each group. $^{*}P < 0.01$, $^{**}P < 0.05$.

DISCUSSION

The present study provided the following three important findings. First, R-ros enhanced Ex4-induced insulin secretion under conditions of high glucose in MIN6B1 cells. Second, in glucose-tolerance tests, the co-administration of R-ros and Ex4 reduced blood glucose levels after glucose injection more markedly than the administration of Ex4 alone in *db/db* mice. Third, long-term treatment with Ex4 and R-ros was more effective for the improvement of HbA1c levels than that with Ex4 alone in *db/db* mice.

Blockers of ATP-sensitive K^+ (K_{ATP}) channels such as sulphonylureas are most widely used to improve hyperglycemia in patients with type 2 diabetes. However, a significant mechanism-based side effect of hypoglycemia is observed in individuals treated with these blockers [26]. The side effect of hypoglycemia has not been reported during monotherapy with Ex4, but it can occur when Ex4 is administered in combination with sulphonylureas [27, 28]. In contrast to sulphonylureas, the insulinotropic effect of Ex4 depends even more closely on the actual glucose concentration, providing the possibility of glucose normalization without the risk of hypoglycemic episodes [15, 25]. R-ros, like Ex4, enhances rapid insulin secretion from pancreatic beta cells in response to elevated glucose concentration and has no effect on insulin secretion under the conditions of low glucose [15]. The present results showed that co-treatment with Ex4 and R-ros enhanced rapid insulin secretion both in vitro and in vivo and had no effect on insulin secretion under conditions of low glucose in MIN6B1 cells. These results suggest that combination therapy with Ex4 and R-ros may have promising therapeutic potential for treating type 2 diabetes without the side effect of hypoglycemia.

db/db mice exhibit biphasic changes of glucose metabolism in an age-dependent manner. The mice initially display hyperinsulinemia, but later hypoinsulinemia because of an impairment of glucose-induced insulin secretion from pancreatic β-cells [21, 22]. The present results showed that co-treatment with Ex4 and R-ros enhanced rapid insulin secretion compared with Ex4 alone in 6-week-old mice, but not in 32-week-old mice. These results suggest that the effect of R-ros may be age- and phase-dependent in patients with type 2 diabetes. It may be important for the application of R-ros for patients that

beta-cells have sufficient capacity for glucose-induced insulin secretion.

In conclusion, R-ros enhanced Ex-4–dependent insulin secretion both acutely and chronically. The co-administration of Ex4 and R-ros is a promising therapy for the treatment of type 2 diabetes.

This work was supported by the Research Program on Development of Innovative Technology from the Japan Science and Technology Agency (JST), by a grant from the New Energy and Industrial Technology Development Organization (NEDO), and by a Grant-in-Aid for Scientific Research on Priority Areas "Membrane Traffic" from the Ministry of Education, Culture, Sports, Science and Technology of Japan.

REFERENCES

1. Leahy JL. Natural history of β-cell dysfunction in NIDDM. Diabetes Care 1990;13:992-1010.
2. Rhodes CJ. Type 2 diabetes-a matter of beta-cell life and death? Science 2005;307:380-4.
3. Henquin JC. The fiftieth anniversary of hypoglycaemic sulphonamides. How did the mother compound work? Diabetologia 1992;35:907-12.
4. Deacon CF. Therapeutic strategies based on glucagon-like peptide 1. Diabetes 2004;53:2181-9.
5. Sturgess NC, Ashford ML, Cook DL, Hales CN. The sulphonylurea receptor may be an ATP-sensitive potassium channel. Lancet 1985;31:474-5.
6. Ashcroft FM, Rorsman P. Electrophysiology of the pancreatic beta-cell. Prog Biophys Mol Biol 1989;54:87-143.
7. Wollheim CB, Lang J, Regazzi R. The exocytotic process of insulin secretion and its regulation by Ca^{2+} and G-proteins. Diabetes Rev 1996;4:276-97.
8. Goke R, Fehmann HC, Linn T et al. Exendin 4 is a high potency agonist and truncated exendin-(9-39)-amide an antagonist at the glucagon-like peptide 1-(7-36)-amide receptor of insulin-secreting beta-cells. J Biol Chem 1993;268:19650-15.
9. Thorens B. Expression cloning of the pancreatic beta cell receptor for the gluco-incretin hormone glucagon-like peptide 1. Proc Natl Acad Sci USA 1992;89:8641-5.
10. Kieffer TJ, McIntosh CH, Pederson RA. Degradation of glucose-dependent insulinotropic polypeptide and truncated glucagon-like peptide 1 in vitro and in vivo by dipeptidyl peptidase IV. Endocrinology 1995;136:3585-96.
11. Siegel EG, Schulze A, Schmidt WE, Creutzfeldt W. Comparison of the effect of GIP and GLP-1 (7-36amide) on insulin release from rat pancreatic islet. Eur J Clin Invest 1992;22:154-7.
12. Alarcon C, Wicksteed B, Rhodes CJ. Exendin 4 controls insulin production in rat islet beta cells predominantly by potentiation of glucose-stimulated proinsulin biosynthesis at the translational level. Diabetologia 2006;49:2920-9.
13. Doyle ME, Egan JM. Mechanisms of action of glucose-like peptide 1 in the pancreas. Pharmacol Ther 2007;113:546-93.
14. Benavides DR, Bibb JA. Role of Cdk5 in drug abuse and plasticity. Ann NY Acad Sci 2004;1025:335-44.
15. Wei FY, Nagashima K, Ohshima T, Saheki Y, Lu YF, Matsushita M, Yamada Y, Mikoshiba K, Seino Y, Matsui H, Tomizawa K. Cdk5-dependent regulation of glucose-stimulated insulin secretion. Nat Med 2005;11:1104-8.
16. Ubeda M, Rukstalis JM, Habener JF. Inhibition of cyclin-dependent kinase 5 activity protects pancreatic beta cells from glucotoxicity. J Biol Chem 2006;281:28858-64.
17. Meijer L, Borgne A, Mulner O, Chong JP, Blow JJ, Inagaki N, Inagaki M, Delcros JG, Moulinoux JP. Biochemical and cellular effects of roscovitine, a potent and selective inhibitor of the cyclin-dependent kinases cdc2, cdk2 and cdk5. Eur J Biochem 1997; 243:527-36.
18. Lilla V, Webb G, Rickenbach K, Maturana A, Steiner DF, Halban PA, Irminger JC. Differential gene expression in well-regulated and dysregulated pancreatic beta-cell (MIN6) sublines. Endocrinology 2003;144:1368-79.
19. Chen H, Charlat O, Tartaglia LA, Woolf EA, Weng X, Ellis SJ, Lakey ND, Culpepper J, Moore KJ, Breitbart RE, Duyk GM, Tepper RI, Morgenstern JP. Evidence that the diabetes gene encodes the leptin receptor: Identification of a mutation in the leptin receptor gene in *db/db* mice. Cell 1996; 84:491–5.
20. Hummel KP, Dickie MM, Coleman DL. Diabetes, a new mutation in the mouse. Science 1966; 53:1127–8.
21. Hunt CE, Lindsey JR, Walkley SU. Animal models of diabetes and obesity, including the PBB/Ld mouse. Fed Proc 1976;35:1206-17.
22. Rodgers BD, Bernier M, Levine MA. Endocrine regulation of G-protein subunit production in an animal model of type 2 diabetes mellitus. J Endocrinol 2001;168:509-15.
23. Buse JB, Henry RR, Han J, Kim DD, Fineman MS, Baron AD. Exenatide-113 Clinical Study Group. Effects of exenatide (exendin-4) on glycemic control over 30 weeks in sulfonylurea-treated patients with type 2 diabetes. Diabetes Care 2004;27:2628-35.
24. Kendall DM, Riddle MC, Rosenstock J, Zhuang D, Kim DD, Fineman MS, Baron AD. Effects of exenatide (exendin-4) on glycemic control over 30 weeks in patients with type 2 diabetes treated with metformin and a sulfonylurea. Diabetes Care 2005;28:1083-91.
25. Ratner RE, Maggs D, Nielsen LL, Stonehouse AH, Poon T, Zhang B, Bicsak TA, Brodows RG, Kim DD. Long-term effects of exenatide therapy over 82 weeks on glycaemic control and weight in over-weight metformin-treated patients with type 2 diabetes mellitus. Diabetes Obes Metab 2006;8:419-28.
26. Moller DE. New drug targets for type 2 diabetes and the metabolic syndrome. Nature 2001;414:821-7.
27. Gallwitz B. Exenatide in type 2 diabetes: treatment effects in clinical studies and animal study data. Int J Clin Pract 2006;60:1654-61.
28. Fineman MS, Bicsak TA, Shen LZ, Taylor K, Gaines E, Varns A, Kim D, Baron AD. Effect on glycemic control of exenatide (synthetic exendin-4) additive to existing metformin and/or sulfonylurea treatment in patients with type 2 diabetes. Diabetes Care 2003;26:2370-7.
29. Alarcon C, Wicksteed B, Rhodes CJ. Exendin 4 controls insulin production in rat islet beta cells predominantly by potentiation of glucose-stimulated proinsulin biosynthesis at the translational level. Diabetologia 2006;49:2920-9.
30. Yusta B, Baggio LL, Estall JL, Koehler JA, Holland DP, Li H, Pipeleers D, Ling Z, Drucker DJ. GLP-1 receptor activation improves beta cell function and survival following induction of endoplasmic reticulum stress. Cell Metab 2006;4:391-406.